



Universidade de Brasília
Instituto de Ciências Exatas
Departamento de Estatística

Dissertação de Mestrado

**Processos de Poisson e o Custo Mínimo Esperado
de Transporte com Sensores**

por

Adolfo Manoel Dias da Silva

Brasília, 03 de junho de 2021

Processos de Poisson e o Custo Mínimo Esperado de Transporte com Sensores

por

Adolfo Manoel Dias da Silva

Dissertação apresentada ao Departamento de Estatística da Universidade de Brasília, como requisito parcial para obtenção do título de Mestre em Estatística.

Orientadora: **Prof^a. Dr^a. Cira Etheowalda Guevara Otiniano**

Brasília, 03 de junho de 2021

Texto aprovado por:

Prof^a Dra. Cira Etheowalda Guevara Otiniano
Orientadora, EST / UnB

Prof. Dr. Antônio Eduardo Gomes
EST / UnB

Prof. Dr. Guilherme Pumi
MAT / UFRGS

Prof. Dr. Guilherme Souza Rodrigues
Suplente, EST / UnB

De tudo ficam três coisas: A certeza de que estamos começando, a certeza de que é preciso continuar e a certeza de que podemos ser interrompidos antes de terminar. Fazer da interrupção um camino novo, fazer da queda um passo de dar, do medo uma escola, do sonho uma ponte, da procura um encontro, e, assim, terá valido a pena existir!

(Fernando Sabino)

Para minha amada família

Meus sinceros agradecimentos aos professores do PPGEST/UnB, em especial, à professora Cira Etheowalda Guevara Otiniano, minha orientadora; à minha família amada e aos meus amigos de turma, Alan da Silva, Thays Suelen, Gustavo e Débora.

O presente trabalho foi realizado com apoio da Coordenação de Aperfeiçoamento de Nível Superior Brasil CAPES Código de Financiamento 001.

Resumo

Neste trabalho, primeiro obtivemos uma fórmula fechada para a distância esperada $E[|X_{k+r} - Y_k|]$ entre eventos de dois processos de Poisson independentes com tempos de chegada X_1, X_2, \dots e Y_1, Y_2, \dots e, respectivas, taxas de chegada λ_1 e λ_2 . Em seguida, foi encontrado um intervalo para a soma $C_{opt} = \sum_{i=1}^n E[|X_i - Y_i|]$. Para o caso particular em que as taxas de chegada dos dois processos λ_1 e λ_2 são iguais a $\lambda > 0$, a fórmula analítica fechada para o custo mínimo esperado de transporte

$$C_{opt}(\lambda, n) = \frac{2n}{3\lambda} \binom{n + \frac{1}{2}}{n},$$

foi determinada por Kranakis (2014).

Como segundo resultado, com o uso da função H de Fox, encontramos o a -ésimo momento absoluto da diferença entre eventos de dois processos de Poisson independentes com tempos de chegadas X_1, X_2, \dots e Y_1, Y_2, \dots e, respectivas taxas λ_1 e λ_2 ,

$$E[|X_{k+r} - Y_k|^a] = \frac{a!(-1)^a}{\lambda_2^a} \sum_{j=0}^a \frac{(k+r)^{(j)}}{j!} \frac{k^{(a-j)}}{(a-j)!} \left(\frac{-\lambda_2}{\lambda_1} \right)^j - 2I_2 \times 1_{[\text{mod}2]}(a),$$

em que

$$I_2 = \frac{(-1)^a (\lambda_1/\lambda_2)^{k+r} \Gamma(a+1) \Gamma(a+r+2k)}{\lambda_2^a \Gamma(k) \Gamma(1+k+r+a)} \times {}_2F_1(a+2k+r; k+r; 1+k+r+a; -\frac{\lambda_1}{\lambda_2}),$$

$$1_{[\text{mod}2]}(a) = \begin{cases} 1, & a \text{ ímpar} \\ 0, & a \text{ par} \end{cases} \quad \text{e} \quad {}_2F_1 \text{ é a função hipergeométrica de Gauss.}$$

Uma potencial aplicação de $C_{opt}(\lambda_1, \lambda_2, n)$ é para o cálculo do custo mínimo de transporte do movimento de sensores alocados conforme os processos $\{X_i, Y_j\}$.

Abstract

In this work, we first obtained a closed formula for the expected distance $E[|X_{k+r} - Y_k|]$ between events of two independent Poisson processes with arrival times X_1, X_2, \dots and Y_1, Y_2, \dots and respective arrival rates λ_1 and λ_2 . Then, a interval was found for the sum $C_{opt} = \sum_{i=1}^n E[|X_k - Y_k|]$. For the particular case, in which the arrival rates of the two processes λ_1 and λ_2 are equal to $\lambda > 0$, the closed analytical formula for the expected minimum cost of transportation

$$C_{opt}(\lambda, n) = \frac{2n}{3\lambda} \binom{n + \frac{1}{2}}{n},$$

was determined by Kranakis (2014).

As a second result, using Fox's H function, we find the absolute a -th absolute moment of difference between events of two independent Poisson processes with arrival times X_1, X_2, \dots and Y_1, Y_2, \dots and, respective rates λ_1 and λ_2 ,

$$E[|X_{k+r} - Y_k|^a] = \frac{a!(-1)^a}{\lambda_2^a} \sum_{j=0}^a \frac{(k+r)^{(j)}}{j!} \frac{k^{(a-j)}}{(a-j)!} \left(\frac{-\lambda_2}{\lambda_1} \right)^j - 2I_2 \times 1_{[\text{mod}2]}(a),$$

where

$$I_2 = \frac{(-1)^a (\lambda_1/\lambda_2)^{k+r} \Gamma(a+1) \Gamma(a+r+2k)}{\lambda_2^a \Gamma(k) \Gamma(1+k+r+a)} \times {}_2F_1(a+2k+r; k+r; 1+k+r+a; -\frac{\lambda_1}{\lambda_2}),$$

$$1_{[\text{mod}2]}(a) = \begin{cases} 1, & a \text{ odd} \\ 0, & a \text{ even} \end{cases} \quad \text{and} \quad {}_2F_1 \text{ is the hypergeometric function.}$$

A potential application of $C_{opt}(\lambda_1, \lambda_2, n)$ is for calculating the minimum cost of transporting the movement of sensors allocated according to the processes $\{X_i, Y_j\}$.

Contents

1	Introdução	1
2	Expected Distance and Interval for Transport Cost	7
2.1	Introduction	7
2.2	Main Results	10
2.2.1	Expected Distance	10
2.3	Minimum expected transport cost	17
2.3.1	Graphic illustrations of C_{opt}	20
2.4	Statistical Inference of C_{opt}	20
2.4.1	Estimation	20
2.4.2	Numerical illustrations	23
2.5	Conclusion	30
3	Generalized moments in Poisson processes	31
3.1	Introduction	31
3.2	Generalized hypergeometric function	32
3.3	Fox's H -function	34
3.4	Main Results	36
3.5	Numerical and Graphical Results	46
3.5.1	Bias of M_k^a	47

3.5.2	Graphic illustrations	50
3.6	Conclusion	53
A	Resultados para o cálculo da integral I_2	55
A.1	Preliminares	55
A.2	Demonstração dos Resultados	56
A.2.1	Resultado $R1$	56
A.2.2	Resultado $R2$	57
A.2.3	Resultado $R3$	58
B	programming code in R	61

Chapter 1

Introdução

Sensores móveis são utilizados no monitoramento e comunicação de dados para diversos fins, como pesquisa oceanográfica (Pérez et al., 2011), análise de ar tropical (Tudose et al., 2011), robótica (Teng et al., 2007), monitoramento e segurança (Ma et al., 2020), entre outros.

Um dos principais tópicos de pesquisa nesta área é a determinação de uma alocação ótima dos sensores de forma a gerar uma boa cobertura a um custo mínimo.

Por meio da tecnologia de sensor móvel, uma boa cobertura pode ser obtida colocando-se os sensores nas posições desejadas. No entanto, os sensores móveis são geralmente equipados com uma bateria e o gasto de energia é muito maior durante o movimento do sensor do que durante sua função de detecção. Portanto, é importante minimizar os movimentos do sensor para aumentar sua vida útil e manter a confiabilidade da rede a que pertence.

Existem duas abordagens para estudar o custo mínimo esperado de transporte: a soma ou o máximo dos movimentos dos sensores desde suas posições iniciais até o destino. Com relação à soma, Ajtai, Komlós, and Tusnády (1984) considerou $2n$ sensores, n azul X_1, X_2, \dots, X_n e n vermelho Y_1, Y_2, \dots, Y_n , distribuídos de forma independente e uniforme em um quadrado unitário e provou que o custo mínimo esperado de transporte, denotado por T_n e definido por $T_n := \min_{\pi} \sum_{i=1}^n d(X_{\pi(i)}, Y_i)$ pertence ao intervalo assintótico $\Theta(\sqrt{n \log n})$. Kranakis (2014), ao assumir que os sensores se movem aleatoriamente em uma reta de acordo com dois processos

de Poisson independentes e identicamente distribuídos com taxas de chegada λ e respectivos tempos de chegada X_1, X_2, \dots, X_n e Y_1, Y_2, \dots, Y_n , determinou um intervalo assintótico para o custo mínimo esperado de transporte $C_T := \sum_{k=1}^n E[|X_k - Y_k|]$. Kapelko (2015) generalizou o resultado do Kranakis (2014). Ele considerou as mesmas hipóteses de Kranakis (2014) e determinou uma expressão assintótica para o custo mínimo esperado, potência $a > 0$, $C_T^a = \sum_{k=1}^n M_{pop}^a$, com $M_{pop}^a = E[|X_k - Y_k|^a]$.

Recentemente, Kapelko (2017), ao considerar dois processos aleatórios gerais idênticos e independentes, determinou expressões assintóticas para o custo mínimo de transporte esperado na potência $b > 0$, C_T^b .

Kapelko (2018) generalizou o resultado de Kranakis (2014), obtendo uma fórmula analítica fechada para o a -ésimo momento da distância absoluta dos tempos de chegada, M_{pop}^a , de dois processos de Poisson i.i.d com taxas λ .

Kapelko (2020) investigou sobre a energia para deslocamento de sensores aleatórios para conectividade e interferência. Para isso, ele determinou M_{pop} entre eventos de processos d -dimensionais, independentes e idênticos com taxas de chegada $\lambda > 0$.

Um problema de custo de transporte mais geral do que os abordados nos artigos citados acima ocorre quando assumimos que os sensores se movem de acordo com dois processos estocásticos, não necessariamente com a mesma distribuição. Nesse trabalho, estudamos este problema mais geral.

Ao considerar, em uma rede de sensores, pares $\{X_i, Y_j\}$, onde X_1, X_2, \dots são azuis e, Y_1, Y_2, \dots são vermelhos, inicialmente colocados de acordo com dois processos de Poisson com taxas $\lambda_1 > 0$ e $\lambda_2 > 0$, respectivamente, estudamos o custo mínimo de transporte esperado, por duas abordagens.

A primeira abordagem, apresentada no Capítulo 2, consiste em determinar um intervalo para C_T . Dessa forma, nossos resultados generalizam os de Kranakis (2014).

O principal resultado com a segunda abordagem, apresentada no Capítulo 3, é uma fórmula

fechada para o a -ésimo momento M_{pop}^a .

No Capítulo 2, iniciamos introduzindo as definições integrais das funções gama, gama incompleta, beta e beta incompleta e identidades envolvendo-as. Em seguida, propomos no Teorema 2.2.1 a seguinte fórmula fechada, em termos da função beta incompleta, para a distância esperada entre eventos de dois processos de Poisson independentes com taxas λ_1 e λ_2 quaisquer:

$$E[|X_{k+r} - Y_k|] = \frac{k+r}{\lambda_1} - \frac{k}{\lambda_2} + 2k(k+r) \binom{2k+r}{k} \left[\frac{B_p(k+r, k+1)}{\lambda_2} - \frac{B_p(k+r+1, k)}{\lambda_1} \right],$$

válida para inteiros $r \geq 0$ e $k \geq 1$, em que $B_p(r, t)$ representa a função beta incompleta com parâmetros $r, t \in \mathbb{N}$ e $p \in (0, 1)$.

Para a demonstração do Teorema 2.2.1, foram necessárias as propriedades de esperança condicional, as funções gama e beta definidas previamente e suas relações com binômios de Newton. Por fim, aplicamos a seguinte identidade combinatória que relaciona a soma polinomial ponderada por coeficientes binomiais com a função beta incompleta (ver DiDonato and Jarnagin, 1966):

$$\sum_{s=0}^L \binom{n+s}{s} p^s = \frac{1-(L+1) \binom{L+n+1}{n} B_p(L+1, n+1)}{(1-p)^{n+1}}.$$

No Corolário 2.2.2, sob as hipóteses de igualdade das taxas e de correspondência entre os tempos de chegadas dos dois processos de Poisson independentes, mostramos a validade da seguinte fórmula:

$$E[|X_k - Y_k|] = \frac{k2^{-2k+1}}{\lambda} \binom{2k}{k}.$$

No Corolário 2.2.3, ao assumir que os processos de Poisson independentes sejam idênticos, obtivemos a mesma fórmula analítica fechada em termos de polinômio de Pochhammer para distância esperada entre os tempos de chegadas X_{k+r} e Y_k apresentada como resultado principal

por Kranakis (2014) :

$$E[|X_{k+r} - Y_k|] = \frac{k2^{-2k+1}}{\lambda} \binom{2k}{k} \left(1 + \sum_{s=0}^{r-1} \frac{r-s}{(2k+s)} \frac{(2k+1)^{(s)}}{2^s (k+1)^{(s)}} \right),$$

A prova deste Corolário foi baseada essencialmente na identidade combinatória que envolve a função beta incompleta regularizada e coeficiente binomial com a aplicação do Princípio da Indução Matemática.

Sob as mesmas hipóteses do Teorema 2.2.1, obtivemos no Teorema 2.3.1 um intervalo para o Custo Mínimo Esperado de Transporte. Demonstramos os limites inferior e superior deste intervalo através de relações de recorrência das funções beta incompletas regularizadas.

No final do Capítulo 2, discutimos a convergência do Custo Amostral. Através de técnicas de inferência estatística, determinamos um intervalo de confiança para o Custo Mínimo de Transporte, após encontrar uma quantidade pivotal baseada no Custo Amostral.

No capítulo 3, tratamos sobre o a -ésimo momento absoluto da diferença entre eventos de dois processos de Poisson. Baseamos nas funções especiais gama, gama incompleta, H -Fox e hipergeométrica de Gauss.

A função H de Fox é bem útil para resolver problemas advindos do cálculo fracionário e solucionar integrais que possuem como integrando as funções gamas. Segundo Mathai, Saxena, and Haubold (2010), a função H de Fox tem grande aplicabilidade em problemas da física, matemática, engenharia e estatística. A sua importância reside no fato de quase todas as funções especiais que ocorrem em matemática e estatística são casos particulares dessa função. A função hipergeométrica de Gauss, por exemplo, é um caso particular da função H de Fox.

Para encontrar o a -ésimo momento, M_{pop}^a , utilizamos as funções especiais H de Fox, hipergeométrica de Gauss, gama, gama incompleta superior e inferior. Essas funções possibilitaram a obtenção de uma fórmula fechada para o a -ésimo momento absoluto da diferença entre os tempos de chegada de dois processos de Poisson independentes.

Apresentamos o Teorema 3.4.1 que generaliza o resultado principal de Kapelko (2018).

Ao considerar dois processos de Poisson independentes com tempos de chegada X_1, X_2, \dots e Y_1, Y_2, \dots e, respectivas taxas λ_1 e λ_2 , mostramos a validade da seguinte fórmula para o a -ésimo momento absoluto:

$$E[|X_{k+r} - Y_k|^a] = \frac{a!(-1)^a}{\lambda_2^a} \sum_{j=0}^a \frac{(k+r)^{(j)}}{j!} \frac{k^{(a-j)}}{(a-j)!} \left(\frac{-\lambda_2}{\lambda_1}\right)^j - 2I_2 \times 1_{[\text{mod}2]}(a),$$

em que

$$I_2 = \frac{(-1)^a (\lambda_1/\lambda_2)^{k+r} \Gamma(a+1) \Gamma(a+r+2k)}{\lambda_2^a \Gamma(k) \Gamma(1+k+r+a)} \times {}_2F_1(a+2k+r; k+r; 1+k+r+a; -\frac{\lambda_1}{\lambda_2}),$$

$$1_{[\text{mod}2]}(a) = \begin{cases} 1, & \text{a ímpar} \\ 0, & \text{a par} \end{cases} \quad \text{e } {}_2F_1 \text{ é a função hipergeométrica.}$$

Para provar o Teorema 3.4.1, demonstramos, primeiramente, os Lemas 3.4.2 e 3.4.3.

No Lema 3.4.2, mostramos a seguinte identidade, válida para todo a inteiro:

$$\int_0^\infty \int_0^\infty (t-y)^a f_2(y) f_1(t) dt dy = \frac{a!(-1)^a}{\lambda_2^a} \sum_{j=0}^a \frac{i^{(j)}}{j!} \frac{k^{(a-j)!}}{(a-j)!} \left(-\frac{\lambda_2}{\lambda_1}\right)^j,$$

onde $f_1(\cdot)$ e $f_2(\cdot)$ são, respectivamente, as densidades das distribuições $Gama(i, \lambda_1)$ e $Gama(k, \lambda_2)$.

No Lema 3.16 mostramos a validade da identidade:

$$I_2 = \frac{\lambda_1^i \lambda_2^k \Gamma(a+1)(-1)^a}{\Gamma(i)\Gamma(k)} \frac{\Gamma(a+i+k)\Gamma(i)}{\Gamma(1+i+a)} \times {}_2F_1(a+i+k, i; 1+i+a; -\frac{\lambda_1}{\lambda_2}),$$

onde $I_2 = \int_0^\infty \int_0^y (t-y)^a f_1(t) f_2(y) dt dy$.

Para sua demonstração, aplicamos as transformadas de Euler e de Laplace da função H de Fox, reduzindo a uma função hipergeométrica.

Para ordem a ímpar, apresentamos o Corolário 3.4.4. Sob as hipóteses do teorema e igual-

dade das taxas de chegadas, obtivemos o resultado apresentado no teorema 3 de Kapelko (2018):

$$E[|X_k - Y_k|^a] = \frac{a!}{\lambda^a} \frac{\Gamma(\frac{a}{2} + k)}{\Gamma(k) \Gamma(\frac{a}{2} + 1)}.$$

Provamos o resultado reescrevendo os polinômios de Pochhammer em função de números binomiais. Aplicamos em seguida, a identidade combinatória e finalizamos colocando a expressão em termos da função gama.

Já para ordem a par, mostramos no Corolário 3.4.5 que nosso resultado coincide com o teorema 9 de Kapelko (2018). Provamos por meio da identidade (Teorema de kummer):

$${}_2F_1(a + 2k, k; 1 + k + a; -1) = \frac{\Gamma(1 + a + 2k - k) \Gamma(1 + \frac{1}{2}(a + 2k))}{\Gamma(1 + a + 2k) \Gamma(1 + \frac{1}{2}(a + 2k) - k)}.$$

Por fim, tanto no Capítulo 2 como no Capítulo 3, inserimos também tabelas e ilustrações gráficas de nossos resultados geradas a partir de simulações dos processos através do software computacional R Core Team (2020). No apêndice A, encontra-se o código da programação.

Chapter 2

Expected Distance and Interval for Transport Cost

2.1 Introduction

Mobile sensors are used in data monitoring and communication for various purposes, such as oceanographic research (Pérez et al., 2011), tropical air analysis (Tudose et al., 2011), robotics (Teng et al., 2007), and security monitoring (Ma et al., 2020), among others.

One of the main research topics in this area is the determination of an optimal allocation of the sensors in order to generate good coverage at a minimum cost.

Through mobile sensor technology, good coverage can be achieved by placing the sensor in the desired positions. However, mobile sensors are generally equipped with a battery and the energy expenditure is much greater during the movement of the sensor than during its detection function. Therefore, it is important to minimize the movements of the sensor to increase its useful life and maintain the reliability of the network to which it belongs.

There are two approaches to studying the minimum expected cost of transport: the sum or maximum of the movements of the sensors from their initial positions to the destination. With respect to the sum, Ajtai, Komlós, and Tusnády (1984) considered $2n$ sensors, n blue

X_1, X_2, \dots, X_n and n red Y_1, Y_2, \dots, Y_n , distributed independently and uniformly in a unit square, and proved that the expected minimum cost of transportation, denoted by T_n and defined by $T_n := \min_{\pi} \sum_{i=1}^n d(X_{\pi(i)}, Y_i)$, belongs to the asymptotic interval $\Theta(\sqrt{n \log n})$. Kranakis (2014), when assuming that the sensors move randomly on a line according to two independent and identically distributed Poisson processes with arrival rate λ and respective arrival times X_1, X_2, \dots and Y_1, Y_2, \dots determined an interval for the expected minimum cost of transport, defined by $C_T = \sum_{k=1}^n E[|X_k - Y_k|]$. Kapelko (2015) generalized the result of Kranakis (2014). He considered the same hypotheses as Kranakis (2014) and determined an asymptotic expression for the expected minimum cost at power $a > 0$, $C_T^a = \sum_{k=1}^n E[|X_k - Y_k|^a]$. Recently, Kapelko (2017), when considering two identical and independent general random processes, determined asymptotic expressions for the expected minimum transport cost at power $b > 0$, C_T^b .

A more general transportation cost problem than that addressed in the articles cited above occurs when it is assumed that the sensors move according to two independent stochastic processes, not necessarily with the same distribution. In this paper, we study this more general problem. Our results generalize Kranakis (2014).

We obtain an exact interval for the transport cost, $C_{opt} = C_T$, by considering a network of two sensors $\{X_i, Y_j\}$, where X_1, X_2, \dots are blue and Y_1, Y_2, \dots are red, that initially randomly allocated according to a Poisson processes with arrival rates $\lambda_1 > 0$ and $\lambda_2 > 0$, respectively. Note that λ_1 can be different from λ_2 , so the sensors $\{X_i\}$ and $\{Y_i\}$ follow a different law. In addition to obtaining an interval for the expected transport cost, here we carry out a study of statistical inference and verify that the sample transport cost is a consistent estimator of the theoretical transport cost found.

Kranakis (2014), Kapelko (2015) and Kapelko (2017) based their results on combinatorial theory, but for the proof of our results we also use results of the following special functions: gamma function, upper and lower incomplete gamma functions, beta function, and incomplete

beta function. These functions are defined, respectively, by:

$$\Gamma(a) := \int_0^\infty t^{a-1} e^{-t} dt, \quad (2.1)$$

$$\Gamma(a, x) := \int_x^\infty t^{a-1} e^{-t} dt, \quad (2.2)$$

$$\gamma(a, x) := \int_0^x t^{a-1} e^{-t} dt, \quad (2.3)$$

$$B(a, b) := \int_0^1 t^{a-1} (1-t)^{b-1} dt \quad (2.4)$$

and

$$B_x(a, b) := \int_0^x t^{a-1} (1-t)^{b-1} dt. \quad (2.5)$$

The following identities (see Gradshteyn and Ryzhik, 2014) are also used:

$$\Gamma(a) = \gamma(a, x) + \Gamma(a, x), \quad (2.6)$$

$$\Gamma(n+1, x) = n! e^{-x} \sum_{r=0}^n \frac{x^r}{r!}, \quad (2.7)$$

$$\gamma(n+1, x) = n! \left(1 - e^{-x} \sum_{r=0}^n \frac{x^r}{r!} \right), \quad (2.8)$$

and

$$\begin{aligned} \frac{\Gamma(x+h)}{\Gamma(x)} &= x^{(h)} : \quad \text{Pochhammer polynomial} \\ &= x(x+1)(x+2) \cdots (x+h-1), \text{ if } h \geq 1. \end{aligned} \quad (2.9)$$

The rest of the chapter is organized as follows: Section 2.2 describes our main results; Section 2.4, presents the statistical inference results about transport cost and illustrations of the results generated from Monte Carlo simulation experiments; and Section 2.5 concludes.

2.2 Main Results

2.2.1 Expected Distance

In this subsection we present Theorem 2.2.1 in which we determine a closed analytic expression for $E[|X_k - Y_k|]$. Let X_i and Y_k be random variables that represent the i -th and k -th arrival times of two independent Poisson processes with rates λ_1 and λ_2 . Then, X_i and Y_k have gamma distribution. With the notation

$$X_i \sim Gama(i, \lambda_1) \quad \text{e} \quad Y_k \sim Gama(k, \lambda_2),$$

the random variables X_i and Y_k have probability density functions (pdf's)

$$f_{X_i}(x) := f_1(x) = \frac{\lambda_1^i}{\Gamma(i)} x^{i-1} e^{-\lambda_1 x}, \quad x > 0 \quad (2.10)$$

and

$$f_{Y_k}(y) := f_2(y) = \frac{\lambda_2^k}{\Gamma(k)} y^{k-1} e^{-\lambda_2 y}, \quad y > 0, \quad (2.11)$$

respectively. The shape parameters are i and k and the scale parameters are $\lambda_1 > 0$ e $\lambda_2 > 0$. The particular cases of our results are in the Corollaries 2.2.2 and 2.2.3. These results correspond to the main results of Kranakis, 2014.

Theorem 2.2.1. *Consider two independent Poisson processes with arrival times X_1, X_2, \dots and Y_1, Y_2, \dots and arrival rates $\lambda_1 > 0$ and $\lambda_2 > 0$, respectively; $\lambda_1 \neq \lambda_2$ or $\lambda_1 = \lambda_2$. Then*

$$E[|X_{k+r} - Y_k|] = \frac{k+r}{\lambda_1} - \frac{k}{\lambda_2} + 2k(k+r) \binom{2k+r}{k} \left[\frac{B_p(k+r, k+1)}{\lambda_2} - \frac{B_p(k+r+1, k)}{\lambda_1} \right], \quad (2.12)$$

for non-negative integers $r \geq 0$ and $k \geq 1$.

Proof. By using the conditional expectation property, we have:

$$\begin{aligned} E[|X_i - Y_k|] &= E[E(|X_i - Y_k| \mid Y_k)] \\ &= \int_0^\infty E[|X_i - y|] f_2(y) dy. \end{aligned} \quad (2.13)$$

To find the the expected value of (2.13), consider:

$$E[|X_i - y|] = I_1 + I_2, \quad \text{with} \quad (2.14)$$

$$I_1 = \int_0^y -(x-y)f_1(x) dx \quad \text{and} \quad I_2 = \int_y^\infty (x-y)f_1(x) dx.$$

By combining (2.10), I_1 and I_2 , we deduce that:

$$I_1 = \frac{\lambda_1^i}{\Gamma(i)} \int_y^\infty x^i e^{-\lambda_1 x} dx - \frac{i}{\lambda_1} + \frac{y\lambda_1^i}{\Gamma(i)} \int_0^y x^{i-1} e^{-\lambda_1 x} dx. \quad (2.15)$$

and

$$I_2 = \frac{\lambda_1^i}{\Gamma(i)} \int_y^\infty x^i e^{-\lambda_1 x} dx - \frac{y \lambda_1^i}{\Gamma(i)} \int_y^\infty x^{i-1} e^{-\lambda_1 x} dx. \quad (2.16)$$

Now (2.15) and (2.16) are replaced in equation (2.14). The expected value result in terms of the incomplete gamma functions is:

$$E[|X_i - y|] = \frac{2}{\lambda_1 \Gamma(i)} \Gamma(i+1, \lambda_1 y) - \frac{i}{\lambda_1} + \frac{y}{\Gamma(i)} (\gamma(i, \lambda_1 y) - \Gamma(i, \lambda_1 y)). \quad (2.17)$$

And by substituting (2.17) in (2.13) we obtain an expression composed of the following three new integrals:

$$E[|X_i - Y_k|] = -\frac{i}{\lambda_1} + \frac{2}{\lambda_1 \Gamma(i)} J_1 + \frac{1}{\Gamma(i)} J_2 - \frac{1}{\Gamma(i)} J_3, \quad (2.18)$$

where

$$\begin{aligned} J_1 &:= \int_0^\infty \Gamma(i+1, \lambda_1 y) f_2(y) dy, \\ J_2 &:= \int_0^\infty y \gamma(i, \lambda_1 y) f_2(y) dy \end{aligned}$$

and

$$J_3 := \int_0^\infty y \Gamma(i, \lambda_1 y) f_2(y) dy.$$

These integrals are calculated using the series representation of the incomplete gamma functions and the density (2.11). After algebraic manipulations, we deduce that:

$$J_1 = \frac{\Gamma(i+1)}{\Gamma(k)} q^k \sum_{s=0}^i \left[p^s \frac{\Gamma(s+k)}{s!} \right], \quad (2.19)$$

$$J_2 = \frac{\Gamma(i)k}{\lambda_2} - \frac{\Gamma(i)}{\lambda_2\Gamma(k)}q^{k+1} \sum_{s=0}^{i-1} \left[p^s \frac{\Gamma(s+k+1)}{s!} \right] \quad (2.20)$$

and

$$J_3 = \frac{\Gamma(i)}{\lambda_2\Gamma(k)}q^{k+1} \sum_{s=0}^{i-1} \left[p^s \frac{\Gamma(s+k+1)}{s!} \right]. \quad (2.21)$$

with $p = \lambda_1/(\lambda_1 + \lambda_2)$ and $q = 1 - p$.

By combining integrals (2.19), (2.20) and (2.21) in (2.18), we get:

$$\begin{aligned} E[|X_i - Y_k|] &= \frac{k}{\lambda_2} - \frac{i}{\lambda_1} + \frac{2i q^k}{\lambda_1\Gamma(k)} \sum_{s=0}^i p^s \frac{\Gamma(s+k)}{s!} - \frac{2q^{k+1}}{\lambda_2\Gamma(k)} \sum_{s=0}^{i-1} p^s \frac{\Gamma(s+k+1)}{s!} \\ &= \frac{k}{\lambda_2} - \frac{i}{\lambda_1} + \frac{2i q^k}{\lambda_1} \sum_{s=0}^i \binom{s+k-1}{s} p^s - \frac{2k q^{k+1}}{\lambda_2} \sum_{s=0}^{i-1} \binom{s+k}{s} p^s, \end{aligned} \quad (2.22)$$

where $p = \lambda_1/(\lambda_1 + \lambda_2)$ and $q = 1 - p$.

Finally, we update equation (2.22), to obtain:

$$\begin{aligned} E[|X_i - Y_k|] &= \frac{k}{\lambda_2} - \frac{i}{\lambda_1} + \frac{2i q^k}{\lambda_1} \left[\frac{1 - (i+1) \binom{i+k}{k-1} B_p(i+1, k)}{q^k} \right] \\ &\quad - \frac{2k q^{k+1}}{\lambda_2} \left[\frac{1 - i \binom{i+k}{k} B_p(i, k+1)}{q^{k+1}} \right] \\ &= \frac{i}{\lambda_1} - \frac{k}{\lambda_2} + 2ik \binom{i+k}{k} \left(\frac{B_p(i, k+1)}{\lambda_2} - \frac{B_p(i+1, k)}{\lambda_1} \right), \end{aligned} \quad (2.23)$$

by using the identity (see DiDonato and Jarnagin, 1966)

$$\sum_{s=0}^L \binom{n+s}{s} p^s = \frac{1-(L+1) \binom{L+n+1}{n} B_p(L+1, n+1)}{(1-p)^{n+1}}. \quad (2.24)$$

Replacing i by $k+r$ in (2.23) finishes the proof. \square

An expression equivalent to (2.12), in terms of the regularized incomplete beta function, is provided below. To obtain this result, just replace the expressions

$$B(k+r, k+1) = \frac{1}{(k+r) \binom{2k+r}{k}} \quad (2.25)$$

and

$$B(k+r+1, k) = \frac{1}{k \binom{2k+r}{k}} \quad (2.26)$$

in the regularized incomplete beta function

$$I_p(a, b) := \frac{B_p(a, b)}{B(a, b)}.$$

Then

$$E[|X_{k+r} - Y_k|] = \frac{k+r}{\lambda_1} - \frac{k}{\lambda_2} + \frac{2k I_p(k+r, k+1)}{\lambda_2} - \frac{2(k+r) I_p(k+r+1, k)}{\lambda_1} \quad (2.27)$$

is equivalent to (2.12).

Corollary 2.2.2. *Consider two independent Poisson processes with arrival times X_1, X_2, \dots and Y_1, Y_2, \dots and arrival rates $\lambda_1 > 0$ and $\lambda_2 > 0$, respectively. If $r = 0$, $k \in \mathbb{Z}_{\geq 1}$ and*

$\lambda_1 = \lambda_2 = \lambda > 0$, then

$$E[|X_k - Y_k|] = \frac{k2^{-2k+1}}{\lambda} \binom{2k}{k}. \quad (2.28)$$

Proof. From Theorem 2.2.1, for $r = 0$ and $p = \lambda_1/(\lambda_1 + \lambda_2) = 1/2$, we have

$$E[|X_{k+r} - Y_k|] = \frac{2k^2}{\lambda} \binom{2k}{k} [B_{\frac{1}{2}}(k, k+1) - B_{\frac{1}{2}}(k+1, k)]. \quad (2.29)$$

The identity

$$B_x(a; n+1-a) = B(a; n+1-a) \sum_{j=a}^n \binom{n}{j} x^j (1-x)^{n-j}, \quad (2.30)$$

(see DiDonato and Jarnagin, 1966), allows rewriting the difference in equation (2.29) as

$$\begin{aligned} B_{\frac{1}{2}}(k, k+1) - B_{\frac{1}{2}}(k+1, k) &= \frac{B(k, k+1)}{2^{2k}} \binom{2k}{k} \\ &= \frac{1}{k2^{2k}}, \end{aligned} \quad (2.31)$$

by using the identity

$$B(k, k+1) = \frac{1}{2k} \binom{2k-1}{k-1}^{-1} = \frac{1}{k} \binom{2k}{k}^{-1}. \quad (2.32)$$

The result (2.28) is obtained replacing (2.31) by (2.29). \square

Corollary 2.2.3. Consider two independent Poisson processes with arrival times X_1, X_2, \dots and Y_1, Y_2, \dots and arrival rates $\lambda_1 > 0$ and $\lambda_2 > 0$, respectively. If $r > 0$, $k \in \mathbb{Z}_{\geq 1}$ and $\lambda_1 = \lambda_2 = \lambda > 0$, then

$$E[|X_{k+r} - Y_k|] = \frac{k2^{-2k+1}}{\lambda} \binom{2k}{k} \left(1 + \sum_{s=0}^{r-1} \frac{r-s}{(2k+s)} \frac{(2k+1)^{(s)}}{2^s} \frac{(k+1)^{(s)}}{(k+1)^{(s)}} \right), \quad (2.33)$$

Proof. For $\lambda_1 = \lambda_2 = \lambda$ and $r > 0$, from Theorem 2.2.1, we have:

$$E[|X_{k+r} - Y_k|] = \frac{r}{\lambda} + \frac{2k(k+r)}{\lambda} \binom{2k+r}{k} [B_{\frac{1}{2}}(k+r, k+1) - B_{\frac{1}{2}}(k+r+1, k)]. \quad (2.34)$$

Equation (2.34) is updated by rewriting $B_{\frac{1}{2}}(k+r, k+1)$ and $B_{\frac{1}{2}}(k+r+1, k)$ with identity (2.30) as

$$\begin{aligned} E[|X_{k+r} - Y_k|] &= \frac{-r}{\lambda} + \frac{2(k+r)}{\lambda 2^k} \sum_{s=0}^{k+r} \binom{s+k-1}{s} \frac{1}{2^s} - \frac{2k}{\lambda 2^{k+1}} \sum_{s=0}^{k+r-1} \binom{s+k}{s} \frac{1}{2^s} \\ &= -\frac{r}{\lambda} + \frac{2(k+r)}{2^k \lambda \Gamma(k)} \times \sum_{j=0}^1 H_j, \end{aligned} \quad (2.35)$$

where

$$\begin{aligned} H_0 &= \sum_{s=0}^{k+r} \frac{(k-1)!}{2^s} \binom{s+k-1}{s} \\ &\stackrel{(s-k:=t)}{=} \Gamma(k) \left[2^{k-1} + 2^{-k} \sum_{t=0}^r \binom{t+2k-1}{k-1} 2^{-t} \right] \end{aligned} \quad (2.36)$$

and

$$\begin{aligned} H_1 &= \sum_{s=0}^{k+r-1} \left(-\frac{1}{k+r} \right) \frac{k!}{2^{s+1}} \binom{s+k}{s} \\ &= -\frac{k!}{2(k+r)} \left[2^k - \binom{2k}{k} 2^{-k} + 2^{-k} \sum_{t=0}^{r-1} \frac{2k+t}{k} \binom{2k+t-1}{k-1} 2^{-t} \right]. \end{aligned} \quad (2.37)$$

By replacing H_0 and H_1 in (2.35), we get:

$$\begin{aligned} E[|X_{k+r} - Y_k|] &= \frac{k 2^{-2k}}{\lambda} \binom{2k}{k} + \frac{2^{-2k+1}}{\lambda} \sum_{t=0}^{r-1} (r-t) \binom{2k+t-1}{k-1} 2^{-t} \\ &\quad + \frac{2^{-2k}}{\lambda} \left[2^{-r} (2k+r) C_{2k+r-1}^{k-1} + \sum_{t=0}^r t \binom{2k+t-1}{k-1} 2^{-t} \right]. \end{aligned} \quad (2.38)$$

Now, the identity

$$\sum_{t=0}^r t \binom{2k+t-1}{k-1} 2^{-t} = 2k \binom{2k-1}{k-1} - 2^{-r} (2k+r) \binom{2k+r-1}{k-1},$$

valid for $k \geq 1$, is applied in (2.38), so:

$$\begin{aligned} E[|X_{k+r} - Y_k|] &= \frac{k2^{-2k}}{\lambda} \binom{2k}{k} + \frac{2^{-2k+1}}{\lambda} \sum_{t=0}^{r-1} (r-t) \binom{2k+t-1}{k-1} 2^{-t} + \frac{k2^{-2k+1}}{\lambda} \binom{2k-1}{k-1} \\ &= \frac{k2^{-2k+1}}{\lambda} \binom{2k}{k} + \frac{2^{-2k+1}}{\lambda} \sum_{t=0}^{r-1} (r-t) \binom{2k+t-1}{k-1} 2^{-t}. \end{aligned} \quad (2.39)$$

Finally, by replacing the binomial identity

$$\binom{2k+s-1}{k-1} = k \binom{2k}{k} \frac{1}{2k+s} \frac{(2k+1)^{(s)}}{(k+1)^{(s)}} \quad (2.40)$$

in (2.39), the result (2.33) is obtained. \square

2.3 Minimum expected transport cost

In this section, we present an interval for the expected transport cost of a pair $\{X_i, Y_k\}$ of sensors placed randomly in the interval $[0, \infty)$. The position of the i -th sensors (blue) and the k -th (red) are determined by the arrival times X_i and Y_k , according to two Poisson process with arrival rates λ_1 and λ_2 , respectively. This expected transport cost corresponds to:

$$C_{opt}(\lambda_1, \lambda_2, n) = \sum_{k=1}^n E[|X_k - Y_k|].$$

Theorem 2.3.1. Consider two independent Poisson processes with arrival times X_1, X_2, \dots and Y_1, Y_2, \dots and arrival rates $\lambda_1 > 0$ and $\lambda_2 > 0$, respectively, such that $\lambda_1 \geq \lambda_2$. Then

$$C_{opt}(\lambda_1, \lambda_2, n) \in [l_n, s_n], \quad (2.41)$$

where

$$l_n = \frac{n(n+1)}{2} \left(\frac{1}{\lambda_1} - \frac{1}{\lambda_2} \right) + \frac{2}{\lambda_2} \times S(n, \lambda_1, \lambda_2), \quad (2.42)$$

$$s_n = \frac{n(n+1)}{2} \left(\frac{1}{\lambda_2} - \frac{1}{\lambda_1} \right) + \left(\frac{1}{\lambda_2} + \frac{1}{\lambda_1} \right) \times S(n, \lambda_1, \lambda_2) \quad (2.43)$$

and

$$S(n, \lambda_1, \lambda_2) = \sum_{k=1}^n \frac{(pq)^k}{B(k+1, k)}. \quad (2.44)$$

Proof. For $r = 0$, from (2.27) we have:

$$E[|X_k - Y_k|] = \frac{k}{\lambda_1} - \frac{k}{\lambda_2} + 2k \left[\frac{I_p(k, k+1)}{\lambda_2} - \frac{I_p(k+1, k)}{\lambda_1} \right]. \quad (2.45)$$

By applying identity

$$I_p(a, b) = I_p(a-1, b+1) - \frac{p^{a-1}q^b}{bB(a, b)},$$

in (2.45), for $a = k+1, b = k$ and $\lambda_1 \geq \lambda_2$, results in:

$$E[|X_k - Y_k|] \geq k \left(\frac{1}{\lambda_1} - \frac{1}{\lambda_2} \right) + 2k \left[\frac{I_p(k, k+1)}{\lambda_2} - \frac{I_p(k+1, k)}{\lambda_2} \right] \quad (2.46)$$

$$= k \left(\frac{1}{\lambda_1} - \frac{1}{\lambda_2} \right) + \frac{2k}{\lambda_2} \frac{(pq)^k}{kB(k+1, k)} \quad (2.47)$$

$$= k \left(\frac{1}{\lambda_1} - \frac{1}{\lambda_2} \right) + \frac{2}{\lambda_2} \frac{(pq)^k}{B(k+1, k)}. \quad (2.48)$$

So, the lower bound of the sum is:

$$\sum_{k=1}^n E[|X_k - Y_k|] \geq \frac{n(n+1)}{2} \left(\frac{1}{\lambda_1} - \frac{1}{\lambda_2} \right) + \frac{2}{\lambda_2} \sum_{k=1}^n \frac{(pq)^k}{B(k+1, k)}, \quad (2.49)$$

To obtain the upper limit of the sum, we replace the identities

$$I_p(a, b) = I_p(a, b + 1) - \frac{p^a q^b}{b B(a, b)}$$

and

$$I_p(a, b) = I_p(a + 1, b) + \frac{p^a q^b}{a B(a, b)}$$

in (2.45). Then, for $a = b = k$, we get:

$$\begin{aligned} \frac{I_p(k, k + 1)}{\lambda_2} - \frac{I_p(k + 1, k)}{\lambda_1} &= \left(\frac{1}{\lambda_2} - \frac{1}{\lambda_1} \right) I_p(k, k) \\ &\quad + \left(\frac{1}{\lambda_2} + \frac{1}{\lambda_1} \right) \frac{(pq)^k}{k B(k, k)}. \end{aligned} \quad (2.50)$$

The upper limit of the sum is obtained from (2.45), (2.50) and the fact that

$I_x(k, k) \leq 1$, $\forall k \in \mathbb{Z}^+$. That is:

$$E[|X_k - Y_k|] \leq k \left(\frac{1}{\lambda_2} - \frac{1}{\lambda_1} \right) + 2 \left(\frac{1}{\lambda_2} + \frac{1}{\lambda_1} \right) \frac{(pq)^k}{B(k, k)} \quad (2.51)$$

and

$$\sum_{k=1}^n E[|X_k - Y_k|] \leq \frac{n(n+1)}{2} \left(\frac{1}{\lambda_2} - \frac{1}{\lambda_1} \right) + \left(\frac{1}{\lambda_2} + \frac{1}{\lambda_1} \right) \sum_{k=1}^n \frac{(pq)^k}{B(k+1, k)}. \quad (2.52)$$

Finally, the proof of Proposition finishes by combining inequalities (2.49) and (2.52). \square

Corollary 2.3.2. Consider two independent Poisson processes with arrival times X_1, X_2, \dots and Y_1, Y_2, \dots and arrival rates $\lambda_1 = \lambda_2 = \lambda$. Then

$$C_{opt}(\lambda, \lambda, n) = \frac{2n}{3\lambda} \binom{n + \frac{1}{2}}{n}. \quad (2.53)$$

Proof. From (2.41), in Theorem 2.3.1, we have

$$\frac{2}{\lambda} \times S(n, \lambda) \leq \sum_{k=1}^n E[|X_k - Y_k|] \leq \frac{2}{\lambda} \times S(n, \lambda).$$

That is

$$\sum_{k=1}^n E[|X_k - Y_k|] = \frac{2}{\lambda} \times S(n, \lambda). \quad (2.54)$$

The proof of (2.53) follows directly from (2.54) and (2.26), because $p = q = 1/2$ and $S(n, \lambda) = \sum_{k=1}^n k 2^{-2k} \binom{2k}{k}$. \square

Equation (2.53) is one of the main results of Kranakis (2014).

2.3.1 Graphic illustrations of C_{opt}

In order to illustrate our results regarding C_{opt} , here we show some graphs of the interval of C_{opt} . These graphs were generated by considering some fixed values of the parameters λ_1 and λ_2 through the Project R for Statistical Computing R Core Team, 2020.

2.4 Statistical Inference of C_{opt}

2.4.1 Estimation

Let $X_i = (X_{i1}, X_{i2}, \dots, X_{im})$ and $Y_i = (Y_{i1}, Y_{i2}, \dots, Y_{im})$; $i \in \{1, 2, \dots, n\}$ be random samples from the Poisson processes with arrival rates λ_1 and λ_2 and respective arrival times

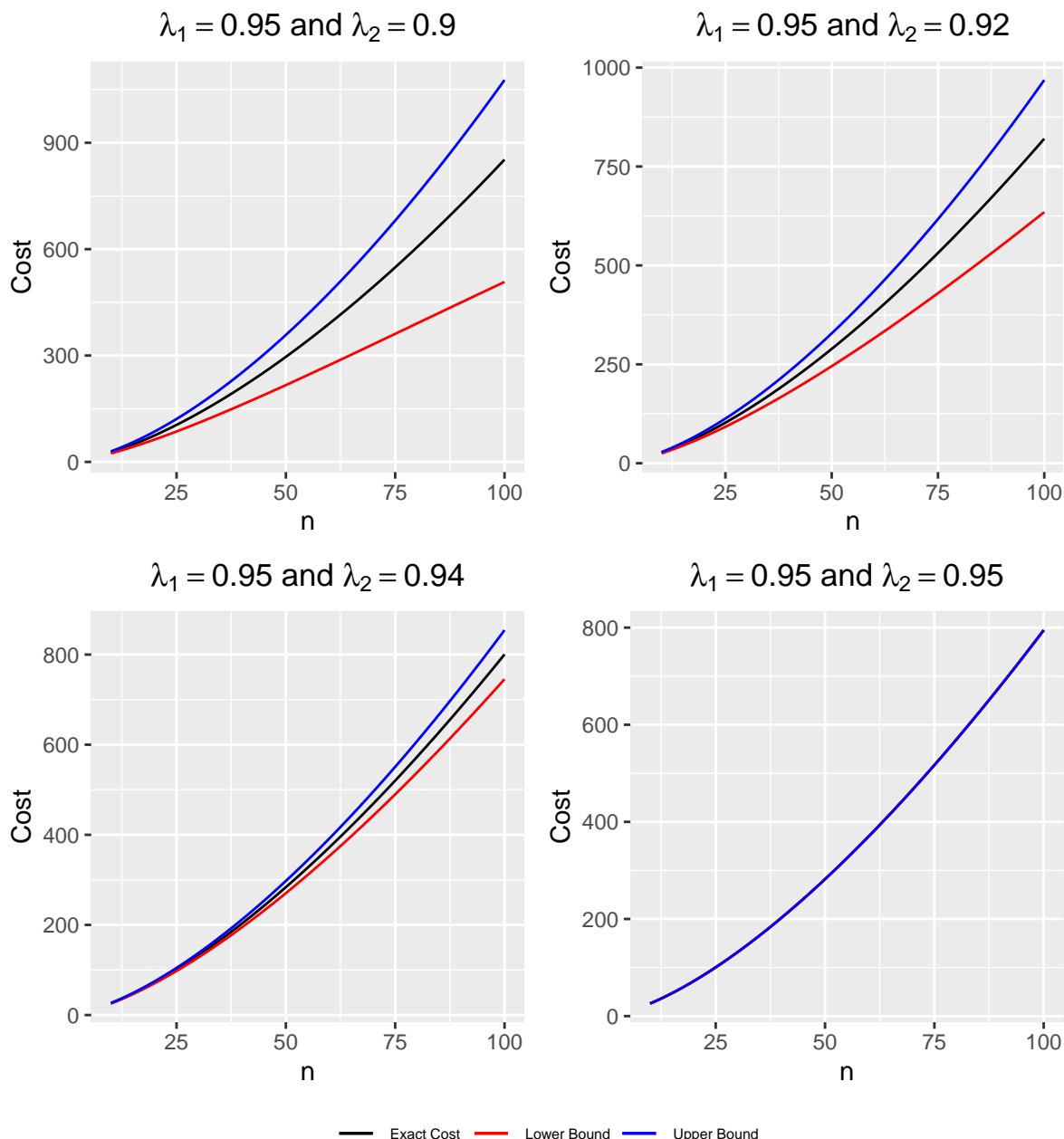


Figure 2.1: Graphs related to the intervals of the minimum expected cost of transport as in (2.41).

X_1, X_2, \dots and Y_1, Y_2, \dots . Then:

$$X_{ij} \sim \text{Gamma}(i, \lambda_1) \text{ and } Y_{ij} \sim \text{Gamma}(i, \lambda_2)$$

for all $(i, j) \in \{1, \dots, n\} \times \{1, \dots, m\}$.

Consider the sample minimum cost

$$\hat{C}_{opt}(n, m) = \frac{1}{m} \sum_{j=1}^m \sum_{i=1}^n |X_{ij} - Y_{ij}|. \quad (2.55)$$

Here, we prove that (2.55) is a good estimator of

$$C_{opt}(\lambda_1, \lambda_2, n)$$

obtained in (2.27). In addition, we prove the asymptotic normality of (2.55) and then define a confidence interval of $C_{opt}(\lambda_1, \lambda_2, n)$.

Since $\left\{ \sum_{i=1}^n |X_{ij} - Y_{ij}| \right\}_{j \geq 1}$ is an infinite sequence of independent and identically distributed (i.i.d.) terms with expected value

$$E[\hat{C}_{opt}(n, m)] = C_{opt}(\lambda_1, \lambda_2, n), \quad (2.56)$$

by the strong law of large numbers, (see Billingsley, 1995) we have that $\hat{C}_{opt}(n, m)$ converges almost surely to the expected value $C_{opt}(\lambda_1, \lambda_2, n)$, that is:

$$\hat{C}_{opt}(n, m) \xrightarrow{a.s.} C_{opt}(\lambda_1, \lambda_2, n), \quad m \rightarrow \infty \quad (2.57)$$

or

$$P \left(\lim_{m \rightarrow \infty} \hat{C}_{opt}(n, m) = C_{opt}(\lambda_1, \lambda_2, n) \right) = 1.$$

Therefore, from (2.56) and (2.57), $\hat{C}_{opt}(n, m)$ is an **unbiased estimator** of $C_{opt}(\lambda_1, \lambda_2, n)$. On the other hand, since the variance

$$Var(\hat{C}_{opt}) = \frac{n(n+1)}{2m} \left(\frac{1}{\lambda_1^2} + \frac{1}{\lambda_2^2} \right) < \infty \quad (2.58)$$

then as m approaches infinity, the sample minimum cost $\hat{C}_{opt}(n, m)$ converges, in distribution, to $N\left(E(\hat{C}_{opt}), Var(\hat{C}_{opt})\right)$. That is:

$$\hat{C}_{opt}(n, m) \xrightarrow{d} N\left(C_{opt}, \frac{n(n+1)}{2m} \left(\frac{1}{\lambda_1^2} + \frac{1}{\lambda_2^2} \right)\right), \quad m \rightarrow \infty. \quad (2.59)$$

From (2.57) and (2.59), we define the confidence interval for $C_{opt}(\lambda_1, \lambda_2, n)$, with confidence coefficient of $1 - \alpha$, by:

$$I_{100(1-\alpha)\%}(C_{opt}) = \left[\hat{C}_{opt} - z_{\alpha/2} \sqrt{Var(\hat{C}_{opt})}, \hat{C}_{opt} + z_{\alpha/2} \sqrt{Var(\hat{C}_{opt})} \right]. \quad (2.60)$$

2.4.2 Numerical illustrations

The performance of statistic (2.55) was tested by Monte Carlo simulation with 10 combinations of λ_1 and λ_2 , as defined in Table 1. We use the algorithm implemented in the computational software R Core Team, 2020, version R 4.0.1 (June, 2020).

Algoritmo 1: Monte Carlo Simulation for Sample Minimum Cost

Input: Rates: λ_1 and λ_2
 Number of Replications: m
 Sizes of Sample (vector): n

Output: Sample Minimum Cost ($\hat{C}_{opt}(n, m)$)

```

1 Function generate.Sample.Cost
2    $\hat{C}_{opt} = []$ 
3   for  $j \leftarrow 1$  to  $\text{length}(n)$  do
4     for  $i \leftarrow 1$  to  $n_j$  do
5        $P_1$ : Generate Random Sample (size= $m$ ) of  $\text{Gamma}(i, \lambda_1)$ ;
6
7        $P_2$ : Generate Random Sample (size= $m$ ) of  $\text{Gamma}(i, \lambda_2)$ .
8     end
9
10     $Dif.Abs :=$  Determine the absolute values of  $(P_2 - P_1)$ ;
11
12     $Mean.Dif :=$  Calculate the means of  $Dif.Abs$ ;
13
14     $Sum.Mean :=$  Add the values of  $Mean.Dif$ .
15  end
16   $\hat{C}_{opt} := Sum.Mean$ .
17  return  $\hat{C}_{opt}$ 
18 end
```

Table 2.1 report the results of the mean estimates of $\hat{C}_{opt}(n, m)$, the values of $C_{opt}(\lambda_1, \lambda_2, n)$ as (2.41), the bias and the mean square error (MSE) of $\hat{C}_{opt}(n, m)$. These results, in Tables 2.1-2.5, confirm the convergence of (2.57). In addition, Figures 2.2a and 2.2b illustrate the good performance of the estimator.

Table 2.1: $C_{opt}(\lambda_1, \lambda_2, n)$, mean estimates, MSE and bias of $\hat{C}_{opt}(n, m)$ with $n = 50$ and $m = 500$.

λ_1	λ_2	$C_{opt}(\lambda_1, \lambda_2, n)$	$\hat{C}_{opt}(n, m)$	MSE	bias
0.55	0.92	951.65	950.02	14.10	-1.63
0.87	0.42	1578.21	1581.17	26.58	2.96
0.59	0.93	816.06	818.44	15.98	2.39
0.70	0.66	404.71	408.61	26.34	3.91
0.86	0.70	451.87	451.46	8.82	-0.41
0.97	0.47	1405.62	1406.26	14.66	0.64
0.43	0.93	1600.54	1598.93	19.33	-1.61
0.87	0.56	841.31	839.06	16.59	-2.26
0.74	0.79	361.95	359.99	12.58	-1.96
0.53	0.90	1007.33	1005.11	17.19	-2.23

Table 2.2: $C_{opt}(\lambda_1, \lambda_2, n)$, mean estimates, MSE and bias of $\hat{C}_{opt}(n, m)$ with $n = 50$ and $m = 1000$.

λ_1	λ_2	$C_{opt}(\lambda_1, \lambda_2, n)$	$\hat{C}_{opt}(n, m)$	MSE	bias
0.55	0.92	951.65	954.80	15.63	3.15
0.87	0.42	1578.21	1579.04	9.60	0.83
0.59	0.93	816.06	819.84	19.49	3.79
0.70	0.66	404.71	408.16	17.46	3.45
0.86	0.70	451.87	449.20	11.45	-2.67
0.97	0.47	1405.62	1406.27	7.56	0.66
0.43	0.93	1600.54	1596.28	26.56	-4.26
0.87	0.56	841.31	837.15	23.09	-4.16
0.74	0.79	361.95	360.87	5.54	-1.08
0.53	0.90	1007.33	1007.90	6.44	0.57

In Table 2.6 we show the results of the confidence interval of $C_{opt}(\lambda_1, \lambda_2, n)$ with 95%, obtained from (2.60). The results are satisfactory. The graphs of these results are shown in Figure 2.3.

Table 2.3: $C_{opt}(\lambda_1, \lambda_2, n)$, mean estimates, MSE and bias of $\hat{C}_{opt}(n, m)$ with $n = 50$ and $m = 1\text{e}4$.

λ_1	λ_2	$C_{opt}(\lambda_1, \lambda_2, n)$	$\hat{C}_{opt}(n, m)$	MSE	bias
0.55	0.92	951.65	951.03	0.95	-0.62
0.87	0.42	1578.21	1577.51	1.38	-0.70
0.59	0.93	816.06	814.87	1.92	-1.19
0.70	0.66	404.71	404.87	0.58	0.16
0.86	0.70	451.87	451.19	0.90	-0.69
0.97	0.47	1405.62	1406.41	1.34	0.79
0.43	0.93	1600.54	1601.29	1.40	0.75
0.87	0.56	841.31	841.84	0.85	0.52
0.74	0.79	361.95	361.81	0.46	-0.13
0.53	0.90	1007.33	1007.02	0.71	-0.31

Table 2.4: $C_{opt}(\lambda_1, \lambda_2, n)$, mean estimates, MSE and bias of $\hat{C}_{opt}(n, m)$ with $n = 50$ and $m = 1\text{e}5$.

λ_1	λ_2	$C_{opt}(\lambda_1, \lambda_2, n)$	$\hat{C}_{opt}(n, m)$	MSE	bias
0.55	0.92	951.65	951.47	0.09	-0.18
0.87	0.42	1578.21	1578.34	0.11	0.14
0.59	0.93	816.06	816.00	0.05	-0.06
0.70	0.66	404.71	404.65	0.06	-0.06
0.86	0.70	451.87	451.57	0.14	-0.30
0.97	0.47	1405.62	1405.99	0.21	0.37
0.43	0.93	1600.54	1601.10	0.40	0.56
0.87	0.56	841.31	841.78	0.27	0.46
0.74	0.79	361.95	361.93	0.04	-0.02
0.53	0.90	1007.33	1007.48	0.08	0.15

Graphically, the result (2.59) is illustrated in Figure 2.4.

Table 2.5: $C_{opt}(\lambda_1, \lambda_2, n)$, mean estimates, MSE and bias of $\hat{C}_{opt}(n, m)$ with $n = 50$ and $m = 1e6$.

λ_1	λ_2	$C_{opt}(\lambda_1, \lambda_2, n)$	$\hat{C}_{opt}(n, m)$	MSE	bias
0.55	0.92	951.65	951.62	0.01	-0.02
0.87	0.42	1578.21	1578.16	0.01	-0.05
0.59	0.93	816.06	816.10	0.01	0.04
0.70	0.66	404.71	404.71	0.01	0.00
0.86	0.70	451.87	451.85	0.00	-0.02
0.97	0.47	1405.62	1405.64	0.01	0.02
0.43	0.93	1600.54	1600.55	0.01	0.01
0.87	0.56	841.31	841.14	0.04	-0.17
0.74	0.79	361.95	361.91	0.01	-0.04
0.53	0.90	1007.33	1007.34	0.01	0.01

Table 2.6: Confidence interval for $C_{opt}(\lambda_1, \lambda_2, n)$ with 95% of confidence.

λ_1	λ_2	$\hat{C}_{opt}(n, m)$	$C_{opt}(\lambda_1, \lambda_2, n)$	$I_{95\%}(C_{opt})$
0.26	0.25	3065.70	3065.53	[3062.16, 3077.46]
0.55	0.28	8801.69	8802.98	[8797.76, 8808.89]
0.91	0.30	11188.47	11188.42	[11184.60, 11194.31]
0.22	0.04	93329.40	93341.57	[93297.73, 93363.09]
0.46	0.90	5389.82	5391.14	[5384.39, 5391.20]
0.78	0.99	1479.48	1478.87	[1477.50, 1482.05]
0.61	0.60	1243.93	1244.34	[1241.60, 1248.07]
0.20	0.56	15906.65	15905.23	[15895.58, 15910.23]
0.20	0.11	20375.64	20375.64	[20366.78, 20395.68]
0.41	0.07	57903.33	57913.29	[57896.82, 57936.20]

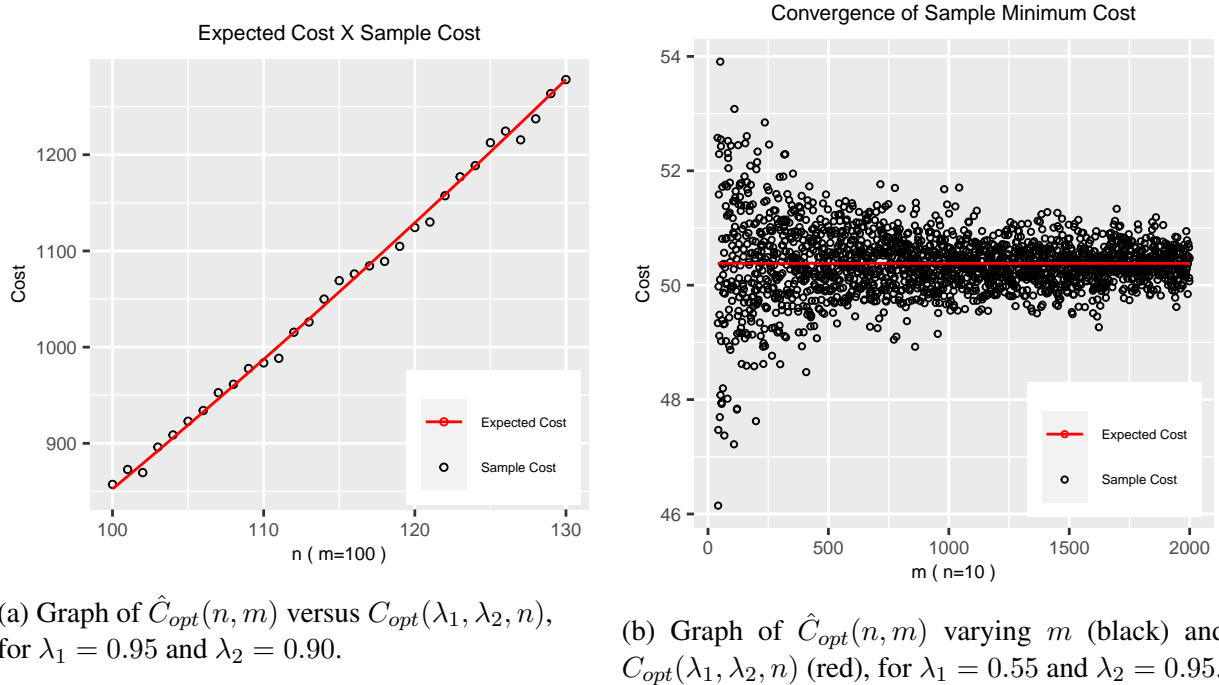


Figure 2.2: Convergence of sample cost

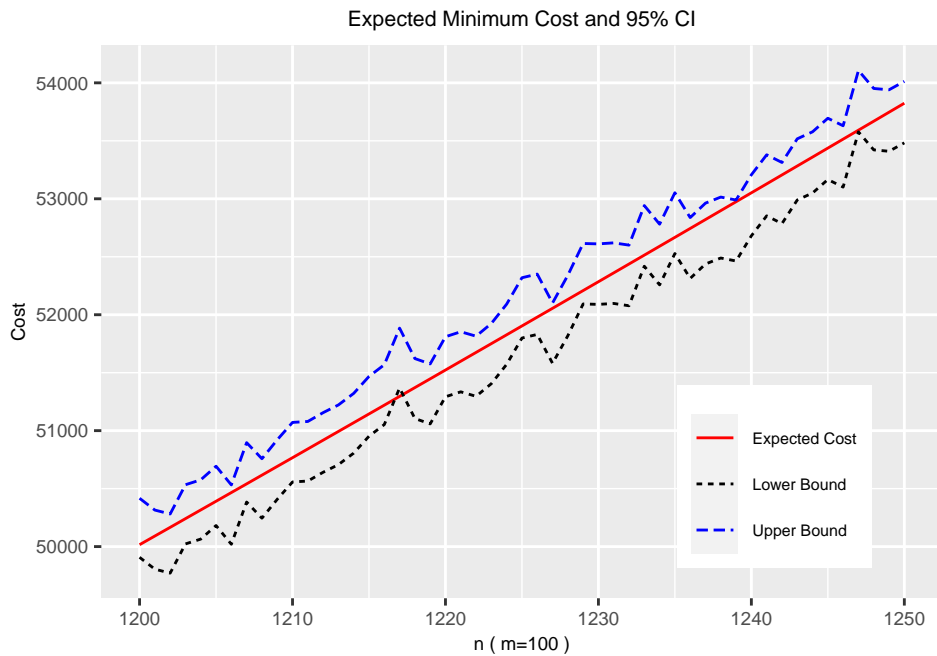


Figure 2.3: Illustration of the confidence interval for $C_{opt}(\lambda_1, \lambda_2, n)$, with 95% of confidence, for $\lambda_1 = 0.95$ and $\lambda_2 = 0.90$.

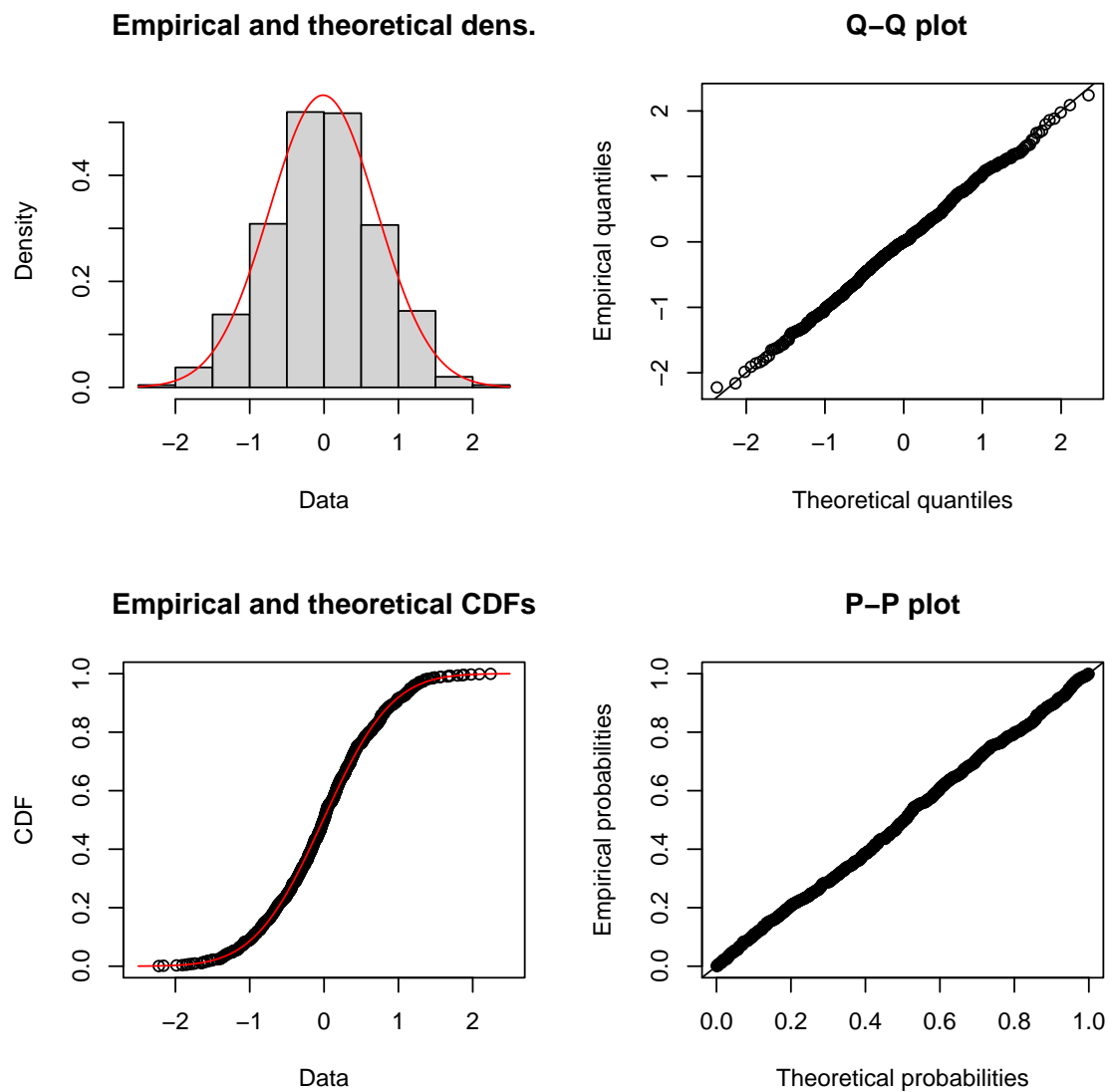


Figure 2.4: Illustration of the asymptotic normality of the estimator $\hat{C}_{opt}(n, m)$ as (2.59).

2.5 Conclusion

In this article, we derive an interval for the sum of the expected absolute difference between two Poisson processes that can have different rates. Our results generalize those of Kranakis (2014), and to apply our results we calculate the minimum transport cost of a random two-color combination when two sensors are initially placed according to two Poisson processes with different or equal laws. We perform a complete statistical inference study, prove asymptotic normality of the cost estimator, and perform a simulation study to show the consistency of the cost estimator.

Chapter 3

Generalized moments in Poisson processes

3.1 Introduction

The problem of determining the cost of moving a sensor, in a network of sensors, measured as the sum or maximum of movements of sensors from their initial positions to target destinations, has been studied by several authors, such as Kranakis (2014). Works related to this subject, considering that the sensors are placed in the network according to a stochastic process, are Ajtai, Komlós, and Tusnády (1984), Kranakis et al. (2013), Kranakis (2014), Kapelko (2018) and Kapelko (2020) and Moltchanov (2012).

Results already available regarding the distance between points of two spatial point processes, the homogeneous Poisson process on \mathbb{R}^2 and the process with points uniformly distributed on \mathbb{R}^2 , were unified by Moltchanov (2012). In the same work, some applications to sensors and mobile wireless networks were also discussed. Some of the papers in which the initial objective is to determine the distance between events of two stochastic processes are Ajtai, Komlós, and Tusnády (1984) and Kranakis et al. (2013). They considered two stochastic processes, in which the arrival times X_1, X_2, \dots and Y_1, Y_2, \dots are independent and uniformly distributed. Kranakis (2014) and Kapelko (2018) derived the expected distance between two independent homogeneous Poisson processes with the same arrival rate and with the respective ar-

rival times X_1, X_2, \dots and Y_1, Y_2, \dots . Recently, Kapelko (2020) investigated about the energy for displacement of random sensors for connectivity and interference. For this, he determined the distance between identical and independent events of d -dimensional Poisson processes with arrival rate $\lambda > 0$.

Further regarding Poisson processes, Kranakis (2014) derived an analytical formula for the absolute distance between arrival times of two independent and identically distributed Poisson processes with arrival rate λ . Kapelko (2018) generalized this result by obtaining a closed analytical formula for the a -th moment of the absolute distance from the arrival times of these same stochastic processes.

In this work, we provide a closed analytical formula for the a -th moment, $E[|X_{k+r} - Y_k|]^a$, by considering two independent Poisson processes, but with any arrival rates, λ_1 and λ_2 and respective arrival times X_1, X_2, \dots and Y_1, Y_2, \dots . We also show that the results of Kapelko (2018) are particular cases of our formulation. In addition, we present numerical illustrations of our result.

The remainder of this paper is structured as follows. In the rest of this section, we present preliminary results of the hypergeometric function and Fox's H -function. In Section 2, we present the main results and, in Section 3, we show numerical results and graphic illustrations .

3.2 Generalized hypergeometric function

In this subsection, we present some basic concepts of the Hypergeometric function and introduce the Fox H -function, which will be useful in the next section.

The generalized hypergeometric function is one of a class of special functions that are very useful in calculating probability. In this article, we use it to show the relationship between our result and Kapelko's results.

According to Srivastava (2019), the generalized hypergeometric function can be defined, in

terms of Pochhammer polynomials,

$$x^{(q)} := \begin{cases} \frac{\Gamma(x+q)}{\Gamma(x)} = x(x+1)\cdots(x+q-1), & q \geq 1 \\ 1, & q = 0, \end{cases} \quad (3.1)$$

by:

$${}_pF_q(a_1, \dots, a_p; b_1, \dots, b_q; z) = \sum_{n=0}^{\infty} \frac{a_1^{(n)} \cdots a_p^{(n)}}{b_1^{(n)} \cdots b_q^{(n)}} \frac{z^n}{n!}, \quad (3.2)$$

where no parameter b_j of the denominator can be zero or a negative integer. Also, If any parameter a_j of the numerator the equation (3.2) is zero or a negative integer, the series ends.

$$\Gamma(\alpha) := \int_0^{\infty} t^{\alpha-1} e^{-t} dt, \quad \alpha > 0$$

is the gamma function.

When $p = 2$ and $q = 1$, a function ${}_pF_q$ is called a hypergeometric function. For the study of ${}_2F_1$, see Oliveira, 2012.

For particular values of z , we have:

1. Case $z = 1$ (Gauss' theorem): Let α, β, ϕ be complex numbers, such that $\operatorname{Re}(\phi - \beta - \alpha) > 0$. So,

$${}_2F_1(\alpha, \beta; \phi; 1) = \frac{\Gamma(\phi) \Gamma(\phi - \alpha - \beta)}{\Gamma(\phi - \alpha) \Gamma(\phi - \beta)}. \quad (3.3)$$

2. Case $z = -1$ (Kummer's theorem): Let α and β be complex numbers, so,

$${}_2F_1(\alpha, \beta; 1 + \alpha - \beta; -1) = \frac{\Gamma(1 + \alpha - \beta) \Gamma(1 + \frac{\alpha}{2})}{\Gamma(1 + \alpha) \Gamma(1 + \frac{\alpha}{2} - \beta)}. \quad (3.4)$$

The computation of the hypergeometric function is available in various programs, including Wolfram Mathematica, Mathematica, Maple and R-Project.

3.3 Fox's H-function

The H function, as introduced by Fox (1961), is a complex contour integral that contains gamma functions in its members (see Mathai, Saxena, and Haubold, 2010), and is defined by:

$$\begin{aligned} H_{p,q}^{m,n}(z) &= H_{p,q}^{m,n} \left[z \left| \begin{matrix} (a_1, A_1), & \dots, & (a_n, A_n), & (a_{n+1}, A_{n+1}), & \dots, & (a_p, A_p) \\ (b_1, B_1), & \dots, & (b_m, B_m), & (b_{m+1}, B_{m+1}), & \dots, & (b_q, B_q) \end{matrix} \right. \right] \\ &= \frac{1}{2\pi i} \int_L \frac{\prod_{j=1}^m \Gamma(b_j + B_j s) \prod_{j=1}^n \Gamma(1 - a_j - A_j s)}{\prod_{j=m+1}^q \Gamma(1 - b_j - B_j s) \prod_{j=n+1}^p \Gamma(a_j + A_j s)} z^{-s} ds, \end{aligned} \quad (3.5)$$

where all A_j and B_j are positive real numbers and all a_j and b_j may be complex numbers. The contour L runs from $c - i\infty$ to $c + i\infty$ such that the poles of $\Gamma(b_j + B_j s)$, $j = 1, \dots, m$ lie to the left of L and the poles of $\Gamma(1 - a_j - A_j s)$, $j = 1, \dots, n$ lie to the right of L .

The H function contains a large number of analytical functions as special cases. Here, we present two special cases of the H function that are useful in proving our main result (see the book by Mathai, Saxena, and Haubold (2010), pages 23 and 24).

$$H_{0\ 1}^{1\ 0} \left[z \left| (\alpha, \beta) \right. \right] = \beta^{-1} z^{\frac{\alpha}{\beta}} e^{-z^{1/\beta}}, \quad (3.6)$$

and

$$H_{2,2}^{1,2} \left[z \left| \begin{matrix} (1-\alpha, 1) & (1-\beta, 1) \\ (0, 1) & (1-\xi, 1) \end{matrix} \right. \right] = \frac{\Gamma(\alpha)\Gamma(\beta)}{\Gamma(\xi)} {}_2F_1(\alpha, \beta; \xi; -z), \quad (3.7)$$

where ${}_2F_1$ is the hypergeometric function. From (3.7), we can verify that the generalized hypergeometric function is a particular case of Fox's H -function.

The H function allows solving different problems arising from probability, physics and engineering, due to its properties and the fact that it has several transforms, such as the Mellin transform, Laplace transform, Laplace inverse transform and Euler transform.

In this work, we use the Laplace transform of $x^{\rho-1} H_{p,q}^{m,n}(\alpha x)$ and the Euler transform of $H_{p,q}^{m,n}(\beta x)$ given, respectively, by:

$$\int_0^\infty e^{-sx} x^{\rho-1} H_{p,q}^{m,n} \left[\alpha x \left| \begin{matrix} (a_p, A_p) \\ (b_q, B_q) \end{matrix} \right. \right] dx = s^{-\rho} H_{p,q}^{m,n} \left[\alpha s^{-\sigma} \left| \begin{matrix} (1-\rho, \sigma) & (a_p, A_p) \\ (b_q, B_q) & \end{matrix} \right. \right] \quad (3.8)$$

and

$$\int_0^x t^{\rho-1} (x-t)^{\sigma-1} H_{p,q}^{m,n}(\beta t^r) dt = \Gamma(\sigma) x^{\rho+\sigma-1} H_{p+1,q+1}^{m,n+1} \left[\beta x^r \left| \begin{matrix} (1-\rho, r) & (a_p, A_p) \\ (b_q, B_q) & (1-\rho-\sigma, r) \end{matrix} \right. \right], \quad (3.9)$$

valid for $\rho \in \mathbb{C}$, $\alpha > 0$, $\sigma > 0$, and $k > 0$. See identity (2.19), pag. 50 and identity (2.51), pag. 58 of (Mathai, Saxena, and Haubold, 2010).

3.4 Main Results

Consider two independent homogeneous Poisson processes with rates λ_1 and λ_2 characterized by the i -th and the k -th arrival times, denoted by X_i and Y_k . Hence, X_i and Y_k are random variables with a gamma distribution, denoted by:

$$X_i \sim \text{Gamma}(i, \lambda_1) \quad \text{and} \quad Y_k \sim \text{Gamma}(k, \lambda_2).$$

So, the probability density functions of these random variables are

$$f_{X_i}(x) := f_1(x) = \frac{\lambda_1^i}{\Gamma(i)} x^{i-1} e^{-\lambda_1 x}, \quad x > 0 \quad (3.10)$$

and

$$f_{Y_k}(x) := f_2(y) = \frac{\lambda_2^k}{\Gamma(k)} x^{k-1} e^{-\lambda_2 y}, \quad y > 0, \quad (3.11)$$

respectively.

Theorem 3.4.1. Consider two independent Poisson processes with arrival rates λ_1 and λ_2 and respective arrival times X_1, X_2, \dots and Y_1, Y_2, \dots . Let $k \geq 1, r \geq 0, a \geq 1$ be integers and $\lambda_1, \lambda_2 > 0$. Then:

$$E[|X_{k+r} - Y_k|^a] = \frac{a!(-1)^a}{\lambda_2^a} \sum_{j=0}^a \frac{(k+r)^{(j)}}{j!} \frac{k^{(a-j)}}{(a-j)!} \left(\frac{-\lambda_2}{\lambda_1}\right)^j - 2I_2 \times 1_{[\text{mod}2]}(a), \quad (3.12)$$

where

$$I_2 = \frac{(-1)^a (\lambda_1/\lambda_2)^{k+r} \Gamma(a+1) \Gamma(a+r+2k)}{\lambda_2^a \Gamma(k) \Gamma(1+k+r+a)} \times {}_2F_1\left(a+2k+r; k+r; 1+k+r+a; -\frac{\lambda_1}{\lambda_2}\right),$$

$$1_{[\text{mod}2]}(a) = \begin{cases} 1, & a \text{ odd} \\ 0, & a \text{ even} \end{cases} \quad \text{and} \quad {}_2F_1 \text{ is the hipergeometric function.}$$

Lemma 3.4.2. Consider the hypotheses of Theorem 3.4.1, a integer and

$$I_1 := \int_0^\infty f_2(y) \int_0^\infty (t-y)^a f_1(t) dt dy.$$

Then, for the $a \geq 1$ integer, the following identity is valid:

$$I_1 = \frac{a!(-1)^a}{\lambda_2^a} \sum_{j=0}^a \frac{i^{(j)}}{j!} \frac{k^{(a-j)!}}{(a-j)!} \left(-\frac{\lambda_2}{\lambda_1} \right)^j. \quad (3.13)$$

Proof. The k -th moment of a random variable $T \sim \text{Gamma}(m, \lambda)$ is given by:

$$\begin{aligned} E(T^k) &= \frac{1}{\lambda^k} \frac{\Gamma(m+k)}{\Gamma(m)} \\ &= \frac{m^{(k)}}{\lambda^k}, \end{aligned} \quad (3.14)$$

using the relation between gamma function and Pochhammer polynomial (3.1). To calculate I_1 we use (3.14) and Newton's binomial

$$\begin{aligned} I_1 &= \int_0^\infty f_2(y) \sum_{j=0}^a \binom{a}{j} (-1)^{a-j} y^{a-j} \frac{i^{(j)}}{\lambda_1^j} dy \\ &= \sum_{j=0}^a \binom{a}{j} (-1)^{a-j} \frac{i^{(j)}}{\lambda_1^j} \int_0^\infty y^{a-j} f_2(y) dy \\ &= \frac{a!}{\lambda_2^a} \sum_{j=0}^a \frac{i^{(j)}}{j!} \frac{k^{(a-j)!}}{(a-j)!} \left(-\frac{\lambda_2}{\lambda_1} \right)^j. \end{aligned} \quad (3.15)$$

□

In the proof of the following lemma we use the theory given in the previous section, about Fox's H -function.

Lemma 3.4.3. Consider the hypotheses of Theorem 3.4.1, $a \geq 1$ integer and

$$I_2 = \int_0^\infty \int_0^y (t-y)^a f_1(t) f_2(y) dt dy.$$

Then, the following identity is valid:

$$I_2 = \frac{\lambda_1^i \lambda_2^k \Gamma(a+1)(-1)^a}{\Gamma(i)\Gamma(k)} \frac{\Gamma(a+i+k)\Gamma(i)}{\Gamma(1+i+a)} {}_2F_1(a+i+k, i; 1+i+a; -\frac{\lambda_1}{\lambda_2}). \quad (3.16)$$

Proof. By replacing (3.10) and (3.11) in I_2 , we get:

$$\begin{aligned} I_2 &= \frac{\lambda_1^i \lambda_2^k}{\Gamma(i)\Gamma(k)} \int_0^\infty y^{k-1} e^{-\lambda_2 y} \left(\int_0^y t^{i-1} (t-y)^a e^{-\lambda_1 t} dt \right) dy \\ &= \frac{\lambda_1^i \lambda_2^k}{\Gamma(i)\Gamma(k)} \int_0^\infty y^{k-1} e^{-\lambda_2 y} (I_{21}) dy. \end{aligned} \quad (3.17)$$

Now, using representation (3.6) for the exponential function of I_{21} , we have:

$$I_{21} = (-1)^a \int_0^y t^{i-1} (y-t)^{(a+1)-1} H_{01}^{10} \left[\lambda_1 t \mid (0, 1) \right] dt. \quad (3.18)$$

Since the integral in (3.18) is an Euler transform of the H function, we use the identity (3.9) and obtain

$$I_{21} = (-1)^a y^{i+a} \Gamma(a+1) H_{12}^{11} \left[\lambda_1 y \mid \begin{matrix} (1-i, 1) \\ (0, 1) \quad (-i-a, 1) \end{matrix} \right]. \quad (3.19)$$

We then update (3.17) by replacing (3.19) in (3.17)

$$I_2 = \frac{\lambda_1^i \lambda_2^k \Gamma(a+1)(-1)^a}{\Gamma(i)\Gamma(k)} \int_0^\infty y^{i+a+k-1} e^{-\lambda_2 y} \left(H_{12}^{11} \left[\lambda_1 y \mid \begin{matrix} (1-i, 1) \\ (0, 1) \quad (-i-a, 1) \end{matrix} \right] \right) dy. \quad (3.20)$$

Finally, since the integral of (3.20) is a Laplace transform of $y^{a+i+k} G_{1\ 2}^{1\ 1}(\lambda_1 y)$, we use identity (3.8) and obtain:

$$I_2 = \frac{\lambda_1^i \lambda_2^k \Gamma(a+1)(-1)^a}{\Gamma(i)\Gamma(k)} \times \\ \times \lambda_2^{-(a+i+k)} H_{2,2}^{1,2} \left[\begin{matrix} (1-a-i-k, 1) & (1-i, 1) \\ (0, 1) & (-i-a, 1) \end{matrix} \middle| \lambda_1 \lambda_2^{-1} \right]. \quad (3.21)$$

The result (3.16) is obtained by using the identity (3.7) in (3.21). \square

Proof. (**Theorem 3.4.1**) By the law of total expectation, we have:

$$E[|X_i - Y_k|^a] = E\left[E[|X_i - Y_k|^a] \middle| Y_k\right] \\ = \int_0^\infty E[|X_i - y|^a] f_2(y) dy. \quad (3.22)$$

The expectation (3.22) is determined for both the odd and even cases, as follows:

When a is even, by definition, we have that

$$E[|X_i - y|^a] = \int_0^\infty (t-y)^a f_1(t) dt \\ = \int_y^\infty (t-y)^a f_1(t) dt + \int_0^y (y-t)^a f_1(t) dt \quad (3.23)$$

Replacing expression (3.23) in (3.22), results in:

$$E[|X_i - Y_k|^a] = I_1. \quad (3.24)$$

Now, we substitute (3.13) in (3.24), with $i = k + r$. Then:

$$E[|X_{k+r} - Y_k|^a] = \frac{a! (-1)^a}{\lambda_2^a} \sum_{j=0}^a \frac{(k+r)^{(j)}}{j!} \frac{k^{(a-j)}}{(a-j)!} \left(-\frac{\lambda_2}{\lambda_1} \right)^j. \quad (3.25)$$

When a is odd, by definition, we have that:

$$\begin{aligned} E[|X_i - y|^a] &= \int_y^\infty (t-y)^a f_1(t) dt + \int_0^y (y-t)^a f_1(t) dt \\ &= \int_0^\infty (t-y)^a f_1(t) dt - 2 \int_0^y (t-y)^a f_1(t) dt. \end{aligned} \quad (3.26)$$

Finally we rewrite (3.22) with (3.26) and obtain:

$$E[|X_i - Y_k|^a] = I_1 - 2I_2. \quad (3.27)$$

The result follows when applying Lemmas 3.4.2 and 3.4.3, equations (3.13) and (3.16) with $i = k + r$. \square

In the next corollaries we show that the identity derived by Kapelko (2018) about the a -th absolute moment of the difference between the arrival times of two identical and independent Poisson processes with rate λ is a particular result of our identity (3.12). Our Corollary 3.4.4 corresponds to Theorem 3 of Kapelko (2018) and our Corollary 3.4.5 corresponds to Theorem 9 of Kapelko (2018).

Corollary 3.4.4. *Consider two identical and independent Poisson processes with arrival rate $\lambda > 0$ and respective arrival times X_1, X_2, \dots and Y_1, Y_2, \dots .*

If $k \geq 1$, $a \geq 1$ are integers with a even, then:

$$E[|X_k - Y_k|^a] = \frac{a!}{\lambda^a} \frac{\Gamma(\frac{a}{2} + k)}{\Gamma(k) \Gamma(\frac{a}{2} + 1)}. \quad (3.28)$$

Proof. For $\lambda_1 = \lambda_2 = \lambda$, from Theorem 3.4.1 follows that

$$\begin{aligned}
 E[|X_k - Y_k|^a] &= \frac{a!}{\lambda_2^a} \sum_{j=0}^a \frac{(k)^{(j)}}{j!} \frac{k^{(a-j)}}{(a-j)!} (-1)^j \\
 &= \frac{a!}{\lambda^a} \sum_{j=0}^a (-1)^j \binom{k-1+j}{j} \binom{k-1+a-j}{a-j} \\
 &= \frac{a!}{\lambda^a} \binom{k-1+a/2}{a/2} \frac{1+(-1)^a}{2}.
 \end{aligned} \tag{3.29}$$

For the last equality (see eq. 3.36; page 40 of Gould, 1972). Equation (3.28) follows from (3.29) when we rewrite the combinations in terms of the gamma function.

□

Corollary 3.4.5. Consider two identical and independent Poisson processes with arrival rate $\lambda > 0$ and respective arrival times X_1, X_2, \dots and Y_1, Y_2, \dots . If $k \geq 1$, $a \geq 1$ are integers with a odd, then:

$$E[|X_k - Y_k|^a] = \frac{a!}{\lambda^a} \frac{\Gamma(\frac{a}{2} + k)}{\Gamma(k) \Gamma(\frac{a}{2} + 1)} \tag{3.30}$$

Proof. Since a is an odd number, from Theorem 3.4.1 we obtain:

$$\begin{aligned}
 E[|X_k - Y_k|^a] &= -2I_2 \\
 &= 2 \frac{\Gamma(a+1)}{\lambda^a \Gamma(k)} \frac{\Gamma(a+2k)}{\Gamma(1+k+a)} \times {}_2F_1(a+2k; k; 1+k+a; -1),
 \end{aligned} \tag{3.31}$$

because,

$$\frac{a!}{\lambda_2^a} \sum_{j=0}^a \frac{(k)^{(j)}}{j!} \frac{k^{(a-j)}}{(a-j)!} (-1)^j = \frac{(-1)^a}{\lambda^a} \sum_{j=0}^a \binom{a}{j} (-1)^j k^{(j)} k^{(a-j)} = 0. \tag{3.32}$$

For identity (3.4), we have that:

$${}_2F_1(a+2k, k; 1+k+a; -1) = \frac{\Gamma(1+a+2k-k) \Gamma(1+\frac{1}{2}(a+2k))}{\Gamma(1+a+2k) \Gamma(1+\frac{1}{2}(a+2k)-k)}. \quad (3.33)$$

The result (3.30) follows when replacing (3.33) in (3.31) and performing some algebraic manipulations. \square

Theorem 3.4.6. Consider two identical and independent Poisson processes with arrival rate $\lambda_1 > 0$ and $\lambda_2 > 0$ and respective arrival times X_1, X_2, \dots and Y_1, Y_2, \dots . If $k \geq 1$, $a \geq 1$ are integers with a odd and $\lambda_2 > \lambda_1$, then:

$$C_{opt}^a = \frac{2a! (-1)^{a+1} \lambda_1 e^{\lambda_1 \lambda_2 / (\lambda_1 + \lambda_2)}}{\lambda_2^a (\lambda_1 + \lambda_2) \Gamma(n)} \Gamma\left(n, \frac{\lambda_1 \lambda_2}{\lambda_1 + \lambda_2}\right). \quad (3.34)$$

Lemma 3.4.7. Let $f_1(\cdot)$ and $f_2(\cdot)$ be the densities of the distributions $\text{Gamma}(i, \lambda_1)$ and $\text{Gamma}(k, \lambda_2)$, respectively, with $a \geq 1$ integer, $\lambda_1 > 0$ and $\lambda_2 > 0$. Then, for $y > 0$:

$$\int_0^\infty \int_0^y (t-y)^a f_1(t) f_2(y) dt dy = \frac{\lambda_1^i \lambda_2^{k-a-i-1} a! (-1)^a}{\Gamma(k)} {}_2F_1(i, a+i+1; a+i+1; -\lambda_1/\lambda_2). \quad (3.35)$$

In particular, when $\lambda_2 > \lambda_1$, you have:

$$I_2 = \frac{(-1)^a a! \lambda_1^i \lambda_2^{k-a-i-1}}{\Gamma(k)} \left(1 + \frac{\lambda_1}{\lambda_2}\right)^{-i}. \quad (3.36)$$

Proof.

$$I_2 := \int_0^\infty \int_0^y (t-y)^a f_1(t) f_2(y) dt dy \quad (3.37)$$

$$= \frac{\lambda_1^i \lambda_2^k}{\Gamma(i)\Gamma(k)} \int_0^\infty \int_0^y (t-y)^a t^{i-1} e^{-\lambda_1 t} y^{k-1} e^{-\lambda_2 y} dt dy \quad (3.38)$$

$$\stackrel{(t=uy)}{=} \frac{\lambda_1^i \lambda_2^k}{\Gamma(i)\Gamma(k)} \int_0^\infty y^{a+i} e^{-\lambda_2 y} \left\{ \int_0^1 (u-1)^a u^{i-1} e^{-\lambda_1 y u} du \right\} dy \quad (3.39)$$

$$= \frac{\lambda_1^i \lambda_2^k}{\Gamma(i)\Gamma(k)} (-1)^a \int_0^\infty y^{a+i} e^{-\lambda_2 y} \underbrace{\left\{ \int_0^1 u^{i-1} (1-u)^a e^{-(\lambda_1 y)u} du \right\}}_{I_{21}} dy. \quad (3.40)$$

Let $I_{21} := \int_0^1 u^{i-1} (1-u)^a e^{-(\lambda_1 y)u} du$.

From the integral representation of the confluent hypergeometric function (see proof of result R1 in the Appendix A)

$${}_1F_1(d; c; x) = \frac{\Gamma(c)}{\Gamma(d)\Gamma(c-d)} \int_0^1 e^{xt} t^{d-1} (1-t)^{c-d-1} dt, \quad (3.41)$$

with $d = i$, $c = a + i + 1$ e $x = -\lambda_1 y$, it follows that

$$I_{21} = \frac{\Gamma(i)\Gamma(a+1)}{\Gamma(a+i+1)} {}_1F_1(i; a+i+1; -\lambda_1 y). \quad (3.42)$$

Replacing the Eq.(3.42) in (3.40), results in

$$I_2 = \frac{\lambda_1^i \lambda_2^k}{\Gamma(i)\Gamma(k)} (-1)^a \int_0^\infty y^{a+i} e^{-\lambda_2 y} \frac{\Gamma(i)\Gamma(a+1)}{\Gamma(a+i+1)} {}_1F_1(i; a+i+1; -\lambda_1 y) dy \quad (3.43)$$

$$= \frac{\lambda_1^i \lambda_2^k (-1)^a}{\Gamma(i)\Gamma(k)} \frac{\Gamma(i)\Gamma(a+1)}{\Gamma(a+i+1)} \underbrace{\int_0^\infty y^{a+i} e^{-\lambda_2 y} {}_1F_1(i; a+i+1; -\lambda_1 y) dy}_{I_{22}}. \quad (3.44)$$

Let $I_{22} := \int_0^\infty y^{a+i} e^{-\lambda_2 y} {}_1F_1(i; a+i+1; -\lambda_1 y) dy$.

From the following result (see proof of result R2 in the Appendix A)

$$\int_0^\infty t^{\mu-1} e^{-xt} {}_1F_1(d; c; qt) dt = \Gamma(\mu) x^{-\mu} {}_2F_1(d, \mu; c; q/x), \quad (3.45)$$

with $d = i$, $c = a+i+1$, $x = \lambda_2$, $\mu = a+i+1$ and $q = -\lambda_1$, follow that

$$I_{22} = \Gamma(a+i+1) \lambda_2^{-(a+i+1)} {}_2F_1(i, a+i+1; a+i+1; -\lambda_1/\lambda_2), \quad (3.46)$$

for $\lambda_1 > 0$ and $\lambda_2 > 0$.

Therefore

$$I_2 = \frac{\lambda_1^i \lambda_2^k (-1)^a}{\Gamma(i)\Gamma(k)} \frac{\Gamma(i)\Gamma(a+1)}{\Gamma(a+i+1)} \Gamma(a+i+1) \lambda_2^{-(a+i+1)} {}_2F_1(i, a+i+1; a+i+1; -\lambda_1/\lambda_2) \quad (3.47)$$

$$= \frac{\lambda_1^i \lambda_2^{k-a-i-1} a! (-1)^a}{\Gamma(k)} {}_2F_1(i, a+i+1; a+i+1; -\lambda_1/\lambda_2). \quad (3.48)$$

And, under the hypothesis that $\lambda_2 > \lambda_1 > 0$, we can find another value for the integral I_2 .

Assuming $\lambda_2 > \lambda_1 > 0$, we have by the result below (see proof of result R3 in the Appendix

A)

$$\int_0^\infty t^{\mu-1} e^{-xt} {}_1F_1(d; \mu; qt) dt = \Gamma(\mu) x^{-\mu} \left(1 - \frac{q}{x}\right)^{-d}, \quad (3.49)$$

with $x = \lambda_2$, $q = -\lambda_1$, $d = i$, and $\mu = a + i + 1$, that

$$I_{22} = \int_0^\infty y^{a+i} e^{-\lambda_2 y} {}_1F_1(i; a+i+1; -\lambda_1 y) dy \quad (3.50)$$

$$= \Gamma(a+i+1) \lambda_2^{-(a+i+1)} \left(1 + \frac{\lambda_1}{\lambda_2}\right)^{-i}. \quad (3.51)$$

Therefore,

$$I_2 = \frac{\lambda_1^i \lambda_2^k}{\Gamma(i) \Gamma(k)} (-1)^a \int_0^\infty y^{a+i} e^{-\lambda_2 y} \frac{\Gamma(i) \Gamma(a+1)}{\Gamma(a+i+1)} {}_1F_1(i; a+i+1; -\lambda_1 y) dy \quad (3.52)$$

$$= \frac{\lambda_1^i \lambda_2^k (-1)^a}{\Gamma(i) \Gamma(k)} \frac{\Gamma(i) \Gamma(a+1)}{\Gamma(a+i+1)} \underbrace{\int_0^\infty y^{a+i} e^{-\lambda_2 y} {}_1F_1(i; a+i+1; -\lambda_1 y) dy}_{I_{22}} \quad (3.53)$$

$$= \frac{\lambda_1^i \lambda_2^k (-1)^a}{\Gamma(i) \Gamma(k)} \frac{\Gamma(i) \Gamma(a+1)}{\Gamma(a+i+1)} \Gamma(a+i+1) \lambda_2^{-(a+i+1)} \left(1 + \frac{\lambda_1}{\lambda_2}\right)^{-i} \quad (3.54)$$

$$= \frac{(-1)^a a! \lambda_1^i \lambda_2^{k-a-i-1}}{\Gamma(k)} \left(1 + \frac{\lambda_1}{\lambda_2}\right)^{-i}. \quad (3.55)$$

□

Proof. (**Theorem 3.4.6**) Considering a odd, we saw that $E[|X_k - Y_k|^a] = -2I_2|_{i=k}$. So, when

$\lambda_2 > \lambda_1 > 0$, it follows that

$$C_{opt}^a = \sum_{k=1}^n E[|X_k - Y_k|^a] \quad (3.56)$$

$$= \frac{2(-1)^{a+1} a!}{\lambda_2^{a+1}} \sum_{k=1}^n \left\{ \frac{\lambda_1^k}{\Gamma(k)} \left(1 + \frac{\lambda_1}{\lambda_2}\right)^{-k} \right\} \quad (3.57)$$

$$= \frac{2 a! (-1)^{a+1}}{\lambda_2^{a+1}} \sum_{k=1}^n \left\{ \frac{1}{\Gamma(k)} \left(\frac{\lambda_1 \lambda_2}{\lambda_1 + \lambda_2}\right)^k \right\} \quad (3.58)$$

$$= \frac{2 a! (-1)^{a+1} \lambda_1 e^{\lambda_1 \lambda_2 / (\lambda_1 + \lambda_2)}}{\lambda_2^a (\lambda_1 + \lambda_2) \Gamma(n)} \Gamma\left(n, \frac{\lambda_1 \lambda_2}{\lambda_1 + \lambda_2}\right). \quad (3.59)$$

□

3.5 Numerical and Graphical Results

For a random sample of size N of each process

$$X_k \sim \text{Gamma}(k, \lambda) \quad \text{e} \quad Y_k \sim \text{Gamma}(k, \lambda),$$

it is natural to consider that the statistic

$$M_k^a = \frac{1}{N} \sum_{j=0}^N |X_{k_j} - Y_{k_j}|^a \quad (3.60)$$

is a moments estimator of

$$\begin{aligned} E[|X_{k+r} - Y_k|^a] &= \frac{a!(-1)^a}{\lambda_2^a} \sum_{j=0}^a \frac{(k+r)^{(j)}}{j!} \frac{k^{(a-j)}}{(a-j)!} \left(\frac{-\lambda_2}{\lambda_1}\right)^j - 2I_2 1_{[\text{mod}2]}(a) \\ &= M_{pop}^a, \end{aligned} \quad (3.61)$$

given in (3.12).

3.5.1 Bias of M_k^a

In this subsection, we present the results obtained, via Monte Carlo simulation, of the bias of M_k^a ; $Bias(M_k^a) = (\frac{1}{m} \sum_{k=1}^m M_k^a) - M_{pop}^a$. The result of the bias is close to zero for different experiments.

We computationally implemented M_{pop}^a in R Core Team (2020), version R 4.0.1 (June, 2020) and simulated m samples of size N of the times X_k and Y_k for each value of $k \in \{1, \dots, 12\}$.

For $\lambda_1 = \lambda_2 = 2$, we simulated $m = 12$ samples of size $N = 1 \times 10^6$, one for each $k \in \{1, \dots, 12\}$. M_{pop}^a , $a = 1, 2, 3, 4$, versus sample moments, M_k^a , $a = 1, 2, 3, 4$. Table 3.2 shows the bias of these sample estimates.

The general case is when $\lambda_1 \neq \lambda_2$. By considering $\lambda_1 = 10$ and $\lambda_2 = 20$ for processes $X_k \sim Gamma(k, \lambda_1)$ e $Y_k \sim Gamma(k, \lambda_2)$, we simulated $m = 12$ samples of size $N = 1 \times 10^7$, one for each $k \in \{1, \dots, 12\}$. The results of the first four population moments and sample moments are shown in Table 3.3 and the bias corresponding to sample estimates is given in Table 3.4.

From the results of Tables 3.2 and 3.4, we can conclude that the statistic (3.60) has a very little bias.

Table 3.1: Population moments versus sample moments for equal rates.

k	M_{pop}^1	M_k^1	M_{pop}^2	M_k^2	M_{pop}^3	M_k^3	M_{pop}^4	M_k^4
1	0.5000	0.5003	0.5000	0.5010	0.7499	0.7527	1.5000	1.5048
2	0.7499	0.7502	1.0000	1.0023	1.8750	1.8826	4.5000	4.5148
3	0.9374	0.9372	1.5000	1.4992	3.2812	3.2787	9.0000	8.9785
4	1.0937	1.0930	2.0000	1.9964	4.9218	4.9017	15.0000	14.8648
5	1.2304	1.2300	2.5000	2.4975	6.7675	6.7529	22.5000	22.4084
6	1.3535	1.3537	3.0000	3.0043	8.7978	8.8340	31.5000	31.7730
7	1.4663	1.4665	3.5000	3.5019	10.9973	11.0109	42.0000	42.1298
8	1.5710	1.5693	4.0000	3.9905	13.3538	13.3086	54.0000	53.7901
9	1.6692	1.6716	4.5000	4.5112	15.8577	15.9202	67.5000	67.9509
10	1.7619	1.7637	5.0000	5.0089	18.5006	18.5418	82.5000	82.7077
11	1.8500	1.8489	5.5000	5.4907	21.2757	21.2321	99.0000	98.8811
12	1.9341	1.9343	6.0000	5.9989	24.1770	24.1542	117.0000	116.7288

Table 3.2: Estimator bias for equal rates.

k	$Bias(M_k^1)$	$Bias(M_k^2)$	$Bias(M_k^3)$	$Bias(M_k^4)$
1	-0.0003	-0.0010	-0.0027	-0.0048
2	-0.0002	-0.0023	-0.0076	-0.0148
3	0.0002	0.0007	0.0025	0.0214
4	0.0006	0.0035	0.0200	0.1351
5	0.0004	0.0024	0.0146	0.0915
6	-0.0002	-0.0043	-0.0361	-0.2730
7	-0.0002	-0.0019	-0.0136	-0.1298
8	0.0017	0.0094	0.0452	0.2098
9	-0.0024	-0.0112	-0.0625	-0.4509
10	-0.0018	-0.0089	-0.0411	-0.2077
11	0.0011	0.0092	0.0436	0.1188
12	-0.0001	0.0010	0.0228	0.2711

Table 3.3: Population moments versus sample moments for different rates.

k	M_{pop}^1	M_k^1	M_{pop}^2	M_k^2	M_{pop}^3	M_k^3	M_{pop}^4	M_k^4
1	0.083	0.083	0.015	0.015	0.004	0.004	0.002	0.002
2	0.137	0.137	0.035	0.035	0.013	0.013	0.006	0.006
3	0.186	0.186	0.060	0.060	0.027	0.027	0.015	0.015
4	0.233	0.233	0.090	0.090	0.046	0.046	0.029	0.029
5	0.280	0.280	0.125	0.125	0.073	0.073	0.051	0.051
6	0.327	0.327	0.165	0.165	0.106	0.106	0.082	0.082
7	0.374	0.374	0.210	0.210	0.148	0.148	0.124	0.124
8	0.421	0.421	0.260	0.260	0.199	0.199	0.179	0.179
9	0.469	0.469	0.315	0.315	0.260	0.260	0.250	0.250
10	0.517	0.516	0.375	0.375	0.331	0.331	0.338	0.338
11	0.565	0.565	0.440	0.440	0.414	0.414	0.447	0.447
12	0.613	0.613	0.510	0.510	0.508	0.508	0.579	0.580

Table 3.4: Estimator bias for different rates.

k	$Bias(M_k^1)$	$Bias(M_k^2)$	$Bias(M_k^3)$	$Bias(M_k^4)$
1	-0.00004	-0.00002	0.00000	0.00000
2	-0.00002	-0.00001	-0.00001	0.00000
3	0.00002	0.00002	0.00002	0.00002
4	-0.00001	0.00000	0.00002	0.00005
5	-0.00003	-0.00001	-0.00001	0.00000
6	0.00010	0.00010	0.00010	0.00020
7	0.00001	0.00002	0.00002	0.00001
8	0.00010	0.00010	0.00010	0.00010
9	-0.00003	-0.00004	-0.00010	-0.00010
10	0.00010	0.00010	0.00010	0.00010
11	-0.00010	-0.00003	0.00004	0.00020
12	-0.00001	-0.00002	-0.00010	-0.00040

Algoritmo 2: Monte Carlo Simulation for Bias and Moments Cost

Input: Arrival Rates: $\lambda_1 > 0$ and $\lambda_2 > 0$.

Arrival Time Vectors k ; Power Vector a and Lag r .

M_p function for calculating the population moment.

Output: Matrices with bias and moment values

```

1 function Moments.Bias
2     Bias:= null matrix with  $n = length(k)$  lines and  $m = length(a)$  columns;
3     Mom:= null matrix with  $n = length(k)$  lines and  $m = 2 * length(a)$  columns.
4
5     for  $i \leftarrow 1$  to  $length(n)$  do
6         Generate  $n$  samples of  $X \sim Gamma(\alpha_i = k_i + r, \lambda_1)$ ;
7         Generate  $n$  samples of  $Y \sim Gamma(k_i, \lambda_2)$ .
8         for  $j \leftarrow 1$  to  $m$  do
9             Mom[ $i, 2j - 1$ ]  $\leftarrow$  Apply the  $M_p$  function at the point  $(a_j, \alpha_i, k_i, r, \lambda_1, \lambda_2)$ 
10            Mom[ $i, 2j$ ]  $\leftarrow$  Calculate the average  $|X - Y|_j^a$ 
11            Bias[ $i, j$ ]  $\leftarrow$  Mom[ $i, 2j - 1$ ] - Mom[ $i, 2j$ ]
12        end
13
14    end
15    Bias ; Mom
16    return Bias matrix and Moments matrix
17 end

```

3.5.2 Graphic illustrations

For each a fixed, $M_{pop}^a = M_{pop}^a(\lambda_1, \lambda_2)$ is a bivariate function. In Figures 3.1 and 3.2, we show its behavior. These graphs were obtained with the aid of packages *ggplot2: Elegant Graphics for Data Analysis*, *gridExtra: Miscellaneous Functions for "Grid" Graphics* and *plot3D: Plotting Multi-Dimensional Data* of software R Core Team (2020), version 4.0.1 (June, 2020)

If $\lambda_1 = \lambda_2 = \lambda$, then the function $M_{pop}^a = M_{pop}^a(\lambda)$ is univariate. Figure 3.1 corresponds to the graph of $M_{pop}^a(\lambda)$ constructed from generating a sequence of 1000 points where $\lambda \in [0.1, 5]$. From this figure, the function decreases faster when a increases.

Graphically, we also show that the function $M_{pop}^a = M_{pop}^a(\lambda_1, \lambda_2)$ is more complex for different rates than for equal rates, because the graph has three dimensions. In order to illustrate the behavior of this function, we fixed the time at $k = 4$, $r = 0$ and allowed λ_1, λ_2 to vary in $[2, 6]$. The graphs of $M_{pop}^a(\lambda_1, \lambda_2)$, generated with 500 points, are shown in Figure 3.2.

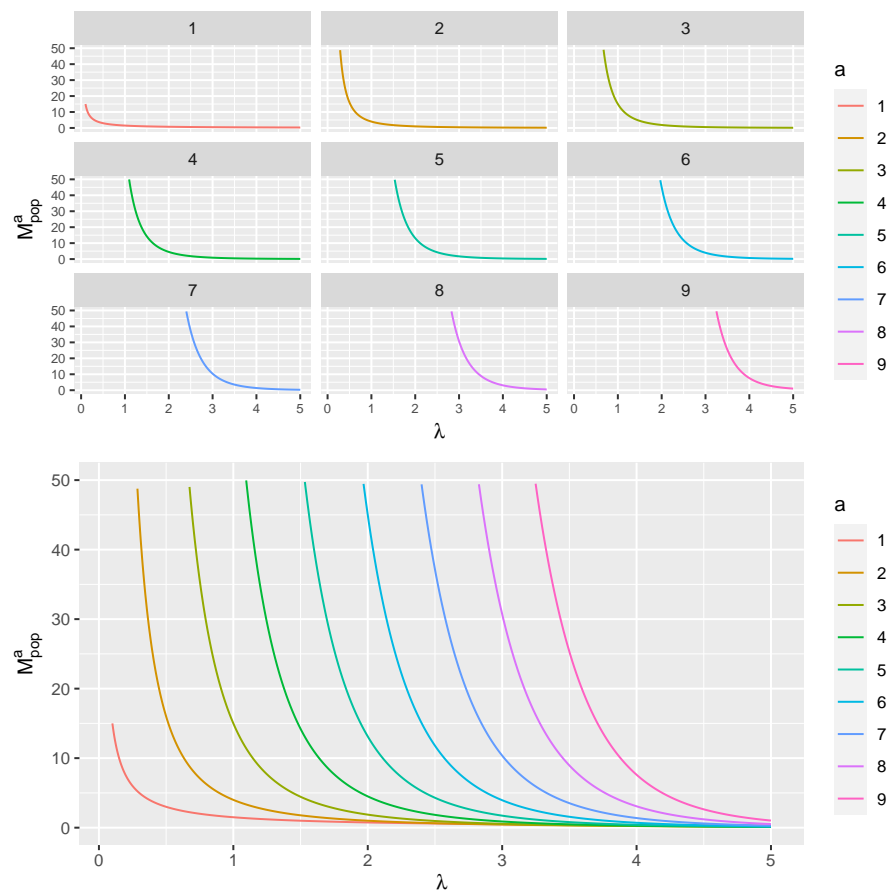


Figure 3.1: Graph of $M^a_{pop}(\lambda)$ for $\lambda \in [0.1, 5]$, $k = 4$ and $r = 0$.

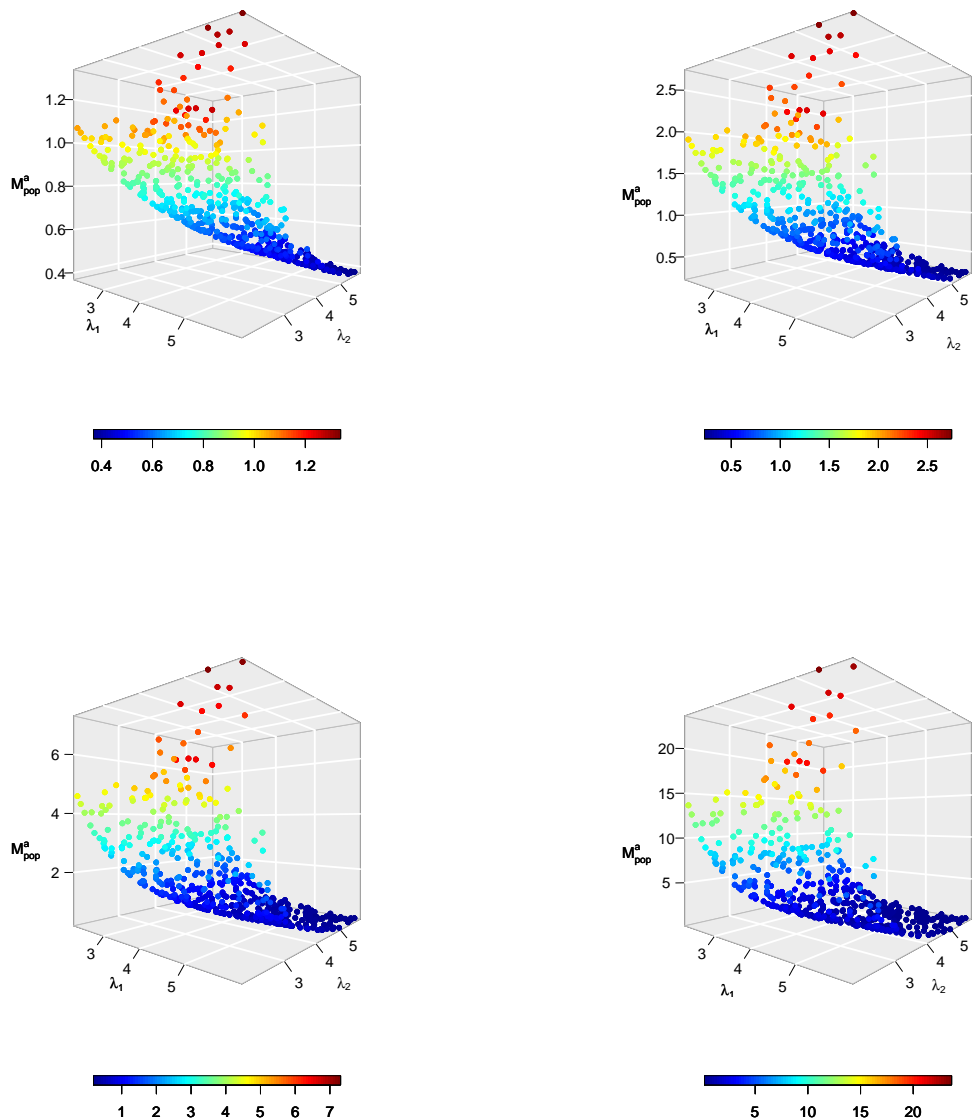


Figure 3.2: Graph of $M_{pop}^a(\lambda_1, \lambda_2)$ for $a = 1, 2, 3, 4$, $k = 4$, $r = 0$, and λ_1, λ_2 in $[2, 6]$.

Algoritmo 3: Generate 3D Graph for population moments

Input: $k \geq 1$ and $r \geq 0$ integers: $\lambda_1 > 0$ and $\lambda_2 > 0$.

λ_1 and λ_2 , generate two random samples of $U(2, 6)$ of size 500.

M_p function for calculating the population moment.

Output: 3D Graph of the $M_{pop}^a(\lambda_1, \lambda_2)$ function of two Poisson processes.

```

1 function 3DGraph
2   Data:=null matrix with  $n = \text{length}(\lambda_1)$  rows and  $m = 4$  columns and a vector
3    $a = (1, 2, 3, 4)$ .
4   for  $i \leftarrow 1$  to  $n$  do
5     for  $j \leftarrow 1$  to  $4$  do
6       Data[ $i, j$ ]  $\leftarrow$  Value of the  $M_p$  at the  $(a_j, k, r, \lambda_{1_i}, \lambda_{2_i})$ 
7     end
8   end
9   for  $t \leftarrow 1$  to  $4$  do
10    Apply the scatter3D function of the plot3D package
11    in the arguments  $(\lambda_1, \lambda_2, Data[*, t], \text{phi} = 0, \text{bty} = "g")$ 
12  end
13  return 3D Graph of the  $M_{pop}^a(\lambda_1, \lambda_2)$ 
14  Remark:  $[*, t] :=$  row by row in column  $t$  of the data matrix
15 end
```

3.6 Conclusion

For independent and identically distributed Poisson processes with rate λ , as commented by Kapelko (2018), it is combinatorially challenging to derive the closed form formula for the $E|X_{k+r} - Y_k|^a$ when a is odd. However, when Fox's H -function is used, in this work, we

show that the proof is direct. In the case that $\lambda_1 > 0$ and $\lambda_2 > 0$ are not necessarily the same, we present here an elegant proof for the expression of the absolute moment of the difference between the arrival times of the two independent Poisson processes. Our results are generalizations of Kapelko (2018). We also present numerical results and graphical illustrations of our results. One possible application is in calculation of the minimum transport cost in a network of two mobile sensors.

Appendix A

Resultados para o cálculo da integral I_2

A.1 Preliminares

Para uma nova solução da integral I_2 , podem ser utilizados os Resultados $R1$, $R2$ e $R3$ abaixo, cujas demonstrações encontram-se no final deste apêndice.

- **$R1$) (Representação Integral da função Hipergeométrica Confluente)**

A seguinte representação é válida

$${}_1F_1(d; c; x) = \frac{\Gamma(c)}{\Gamma(d)\Gamma(c-d)} \int_0^1 e^{xt} t^{d-1} (1-t)^{c-d-1} dt, \quad (\text{A.1})$$

onde $\mathcal{R}(c) > \mathcal{R}(d) > 0$.

- **$R2$) (Transformada de Laplace de uma função Hipergeométrica Confluente)**

A seguinte identidade é válida

$$\int_0^\infty t^{\mu-1} e^{-xt} {}_1F_1(d; c; qt) dt = \Gamma(\mu) x^{-\mu} {}_2F_1(d, \mu; c; q/x). \quad (\text{A.2})$$

onde $\mathcal{R}(x) > 0$, $\mathcal{R}(x) > \mathcal{R}(q)$, $\mathcal{R}(\mu) > 0$ e ${}_2F_1$ é uma função hipergeométrica.

- R3) (Caso Particular do Resultado R2, para parâmetros c e μ iguais)

$$\int_0^\infty t^{\mu-1} e^{-xt} {}_1F_1(d; \mu; qt) dt = \Gamma(\mu) x^{-\mu} \left(1 - \frac{q}{x}\right)^{-d}, \quad (\text{A.3})$$

onde $\mathcal{R}(x) > \mathcal{R}(q)$, $|x| > |q|$, $\mathcal{R}(\mu) > 0$ e ${}_1F_1$ é uma função hipergeométrica confluente.

Para o estudo das funções hipergeométrica ${}_2F_1$ e hipergeométrica confluente ${}_1F_1$, adotamos a referência Oliveira (2012). Nesta, a primeira função encontra-se no Capítulo 5 e, a segunda, no Capítulo 8.

A.2 Demonstração dos Resultados

A.2.1 Resultado R1

A seguinte representação é válida

$${}_1F_1(d; c; x) = \frac{\Gamma(c)}{\Gamma(d)\Gamma(c-d)} \int_0^1 e^{xt} t^{d-1} (1-t)^{c-d-1} dt, \quad (\text{A.4})$$

onde $\mathcal{R}(c) > \mathcal{R}(d) > 0$.

Proof. Da representação integral associada à função Hipergeométrica:

$${}_2F_1(d, b; c; z) = \frac{\Gamma(c)}{\Gamma(c-b)\Gamma(b)} \int_0^\infty t^{b-1} (1-t)^{c-b-1} (1-zt)^{-d} dt, \quad (\text{A.5})$$

com $\mathcal{R}(c) > \mathcal{R}(b) > 0$, decorre que, considerando a mudança de variável $z = x/b$,

$${}_2F_1(d, b; c; x/b) = \frac{\Gamma(c)}{\Gamma(c-b)\Gamma(b)} \int_0^1 t^{b-1} (1-t)^{c-b-1} \left(1 - \frac{xt}{b}\right)^{-d} dt. \quad (\text{A.6})$$

Agora, tomando o limite para $b \rightarrow \infty$, em A.6, obtemos

$${}_1F_1(d; c; x) = \frac{\Gamma(c)}{\Gamma(d)\Gamma(c-d)} \int_0^1 e^{xt} t^{d-1} (1-t)^{c-d-1} dt. \quad (\text{A.7})$$

□

A.2.2 Resultado R2

Mostre que

$$\int_0^\infty t^{\mu-1} e^{-xt} {}_1F_1(d; c; qt) dt = \Gamma(\mu) x^{-\mu} {}_2F_1(d, \mu; c; q/x). \quad (\text{A.8})$$

onde $\mathcal{R}(x) > 0$, $\mathcal{R}(x) > \mathcal{R}(q)$, $\mathcal{R}(\mu) > 0$ e ${}_2F_1$ é uma função hipergeométrica.

Proof. Para a prova, utilizaremos as representações em séries de potência para as funções hipergeométrica confluente e hipergeométrica.

Com efeito, pela representação em séries de potência, decorre que

$$\int_0^\infty t^{\mu-1} e^{-xt} {}_1F_1(d; c; qt) dt = \int_0^\infty t^\mu e^{-xt} \left\{ \sum_{n=0}^\infty \frac{d^{(n)}}{c^{(n)}} \frac{(qt)^n}{n!} \right\} dt \quad (\text{A.9})$$

$$= \frac{\Gamma(c)}{\Gamma(d)} \int_0^\infty t^{\mu-1} e^{-xt} \left\{ \sum_{n=0}^\infty \frac{\Gamma(d+n)}{\Gamma(c+n)} \frac{(qt)^n}{n!} \right\} dt \quad (\text{A.10})$$

$$= \frac{\Gamma(c)}{\Gamma(d)} \sum_{n=0}^\infty \left\{ \frac{\Gamma(d+n)}{\Gamma(c+n)} \frac{q^n}{n!} \underbrace{\int_0^\infty t^{\mu+n-1} e^{-xt} dt}_{\text{Núcleo Gamma}(\mu+n, x)} \right\} \quad (\text{A.11})$$

$$= \frac{\Gamma(c)}{\Gamma(d)} \sum_{n=0}^\infty \left\{ \frac{\Gamma(d+n)q^n}{\Gamma(c+n)} \frac{\Gamma(\mu+n)}{x^{\mu+n}} \right\} \quad (\text{A.12})$$

$$= \Gamma(\mu)x^{-\mu} \underbrace{\frac{\Gamma(c)}{\Gamma(d)\Gamma(\mu)} \sum_{n=0}^\infty \frac{\Gamma(d+n)\Gamma(\mu+n)}{\Gamma(c+n)} \frac{(q/x)^n}{n!}}_{{}_2F_1(d, \mu; c; q/x)} \quad (\text{A.13})$$

$$= \Gamma(\mu)x^{-\mu} {}_2F_1(d, \mu; c; q/x), \quad (\text{A.14})$$

em que a igualdade na Eq.(A.27) é justificada pela representação em séries de potência da função hipergeométrica confluente e, a passagem da Eq.(A.31) para a Eq.(A.32), pela representação em séries de potência da hipergeométrica. \square

A.2.3 Resultado R3

Mostre que

$$\int_0^\infty t^{\mu-1} e^{-xt} {}_1F_1(d; \mu; qt) dt = \Gamma(\mu)x^{-\mu} \left(1 - \frac{q}{x}\right)^{-d}, \quad (\text{A.15})$$

onde $\mathcal{R}(x) > \mathcal{R}(q)$, $|x| > |q|$, $\mathcal{R}(\mu) > 0$ e ${}_1F_1$ é uma função hipergeométrica confluente.

Proof. De fato, da representação em séries para função hipergeométrica confluente, tem-se

$$\int_0^\infty t^{\mu-1} e^{-xt} {}_1F_1(d; \mu; qt) dt = \frac{\Gamma(\mu)}{\Gamma(d)} \int_0^\infty t^{\mu-1} e^{-xt} \left\{ \sum_{n=0}^\infty \frac{\Gamma(d+n)}{\Gamma(\mu+n)} \frac{(qt)^n}{n!} \right\} dt \quad (\text{A.16})$$

$$= \frac{\Gamma(\mu)}{\Gamma(d)} \sum_{n=0}^\infty \left\{ \frac{\Gamma(d+n)}{\Gamma(\mu+n)} \frac{q^n}{n!} \int_0^\infty t^{n+\mu-1} e^{-xt} dt \right\} \quad (\text{A.17})$$

$$= \frac{\Gamma(\mu)}{\Gamma(d)} \sum_{n=0}^\infty \left\{ \frac{\Gamma(d+n)}{\Gamma(\mu+n)} \frac{q^n}{n!} \frac{\Gamma(\mu+n)}{x^{\mu+n}} \right\} \quad (\text{A.18})$$

$$= \Gamma(\mu) x^{-\mu} \sum_{n=0}^\infty \frac{\Gamma(d+n)}{\Gamma(d)} \frac{(q/x)^n}{n!} \quad (\text{A.19})$$

$$= \Gamma(\mu) x^{-\mu} \sum_{n=0}^\infty \binom{n+d-1}{n} (q/x)^n \quad (\text{A.20})$$

$$= \Gamma(\mu) x^{-\mu} \left(1 - \frac{q}{x}\right)^{-d}, \quad (\text{A.21})$$

em que, na passagem da Eq.(A.38) para Eq.(A.39), usamos a identidade combinatória

$$(1-h)^{-d} = \sum_{n \geq 0} \binom{n+d-1}{d-1} h^n. \quad (\text{A.22})$$

□

Appendix B

programming code in R

```
1 #=====
2 ##### Custo Minimo Esperado (Kranakis [2014]) #####
3 #####
4 ## Funcao Distancia Esperada
5 E0<-function(k,l) { (k*2^(-2*k+1)/l)*choose(2*k,k) }
6 ## Grafico para o Custo Minimo Esperado
7 Graf_Int.Custo0<-function(n,l) {
8     L<-length(n)
9     custo<-LI<-LS<-numeric(L)
10    for (j in 1:L) {
11        LI[j]<-(n[j]*n[j]^0.5)/(2*exp(1)*(2*pi)^0.5*l)
12        LS[j]<-(2*exp(1/24)*n[j]*n[j]^0.5)/(pi^0.5*l)
13        custo[j]<-sum(E0(1:n[j],l))
14    }
15    plot(n,custo,type="l", # Plote do Custo
16          main="Custo Minimo Esperado",
17          ylab=expression(C(n,lambda)))
18    lines(n,LI,col="red") # Limite Inferior
```

```

19   lines(n,LS,col="blue") # Limite Superior
20 }
21 ## Plote dos Graficos
22 l<-c(0.35,0.55,0.75,0.95) ; x11() ; par(mfrow=c(2,2))
23 for (i in 1:4){
24   Graf_Int.Custo0(v,l[i])
25   legend("topleft", legend=bquote(lambda==.(l[[i]])))
26 }
27 ##### CUSTO GENERALIZADO #####
28 ##### Funcao Distancia Esperada
29
30 ## Grafico para o Custo Generalizado
31 E<-function(k,l1,l2){
32   x<-l1/(l1+l2)
33   res<-k*(1/l1-1/l2)+2*k*((1/l2)*pbeta(x,k,k+1)-(1/l1)*pbeta(x,k+1,k))
34   return(res)
35 }
36
37 Graf_Int.Custo<-function(n,l1,l2){
38   L<-length(n) ; x<-l1/(l1+l2) ; y<-1-x
39   custo<-LI<-LS<-numeric(L)
40   for (i in 1:L) {
41     LI[i]<-(n[i]*(n[i]+1)/2)*(1/l1-1/l2)+(2/l2)*
42           sum((x*y)^(1:n[i]))/beta(1:n[i]+1,1:n[i]))
43     LS[i]<-(n[i]*(n[i]+1)/2)*(1/l2-1/l1)+(1/l2+1/l1)*
44           sum(((x*y)^(1:n[i]))/beta(1:n[i]+1,1:n[i])))
45     custo[i]<-sum(E(1:n[i],l1,l2))
46   }

```

```

47 plot(n,custo,type="l",main="Custo Minimo Esperado",
48       ylab=expression(C(n,lambda[1],lambda[2])))
49 lines(n,LI,col="red") ; lines(n,LS,col="blue")
50 }
51 ## Plote dos Graficos
52 v<-seq(10,100,1)
53 l1<-rep(0.95,4)
54 l2<-c(0.90,0.92,0.94,0.95)
55 x11(); par(mfrow=c(2,2))
56 for (i in 1:4) {
57   Graf_Int.Custo(v,l1[i],l2[i])
58   legend("topleft", legend=bquote(lambda[1]==.(l1[[i]]) ~ ",
59                                     lambda[2]==.(l2[[i]])) )
60 }
61 #=====
62 #=====DISTANCIA ESPERADA E CUSTO TEORICO (EXATO) =====#
63 #=====
64 E<-function(k,l1,l2){
65   x<-l1/(l1+l2)
66   res<-k*(1/l1-1/l2)+2*k*((1/l2)*pbeta(x,k,k+1)-(1/l1)*pbeta(x,k
67   +1,k))
68   return(res)
69 }
70 Custo_teorico<-function(n,l1,l2){
71   custo<-numeric(length(n))
72   for (j in 1:length(n)){
73     custo[j]<-sum(E(1:n[j],l1,l2)) }
74 return(custo)

```

```

74 }
75 #=====
76 #===== GRAFICO CUSTO TEORICO =====#
77 #=====#
78 G_Int<-function(n,l1,l2) {
79   L<-length(n)
80   x<-l1/(l1+l2)
81   y<-1-x
82   custo<-LI<-LS<-numeric(L)
83   for (i in 1:L) {
84     LI[i]<- (n[i] * (n[i]+1)/2) * (1/l1-1/l2)+(2/l2) *
85       sum((x*y)^(1:n[i])) /beta(1:n[i]+1,1:n[i]))
86     LS[i]<- (n[i] * (n[i]+1)/2) * (1/l2-1/l1)+(1/l2+1/l1) *
87       sum(((x*y)^(1:n[i]))) /beta(1:n[i]+1,1:n[i]))
88     custo[i]<-sum(E(1:n[i],l1,l2))
89   }
90   plot(n,custo,type="l",main="Expected Minimum Cost",
91         ylab=expression(C[opt](n,lambda[1],lambda[2])),
92         cex.main=0.75,cex=0.4,cex.lab=.7,cex.axis=0.7)
93   lines(n,LI,col="red") ; lines(n,LS,col="blue")
94 }
95 v<-seq(10,100,1)
96 l1<-rep(0.95,4)
97 l2<-c(0.90,0.92,0.94,0.95)
98 x11(width = 3.8, height=4.5)
99 par(mfrow=c(2,2))
100 for (i in 1:4) {
101   G_Int(v,l1[i],l2[i])

```

```

102 legend("topleft", legend=bquote(lambda[1]==.(l1[[i]]) ~ ", " ~ lambda
103 [2]==.(l2[[i]])),cex=0.42)
104
105 legend("bottomright",inset=0.02,legend=c("Upper Bound","Exact Cost",
106 "Lower Bound"),col=c("blue","black","red"),lty=c(1,1),cex=0.33)
107 }
108
109 ## GG PLOT2
110
111 Int<-function(n,l1,l2){
112   L<-length(n) ; x<-l1/(l1+l2) ; y<-1-x
113   custo<-LI<-LS<-numeric(L)
114   for (i in 1:L) {
115     LI[i]<-(n[i]*(n[i]+1)/2)*(1/l1-1/l2)+(2/l2)*
116     sum((x*y)^(1:n[i]))/beta(1:n[i]+1,1:n[i]))
117     LS[i]<-(n[i]*(n[i]+1)/2)*(1/l2-1/l1)+(1/l2+1/l1)*
118     sum(((x*y)^(1:n[i]))/beta(1:n[i]+1,1:n[i]))
119     custo[i]<-sum(E(1:n[i],l1,l2))
120   }
121   df<-data.frame(Linf=LI, Custo=custo, Lsup=LS)
122   return(df)
123 }
124
125 v<-seq(10,100,1)
126 l1<-rep(0.95,4)
127 l2<-c(0.90,0.92,0.94,0.95)
128
129 list.df<-list()
130 for (i in 1:4) {
131   list.df[[i]]<-Int(v,l1[i],l2[i])
132 }
133
134 library(ggplot2)
135
136 graf<-list()

```

```

128 df.new<-list()
129 for (i in 1:4) {
130   l<-l1[i] ; u<-l2[i]
131   df.new[[i]]<-data.frame(v,list.df[i])
132 }
133 p2<-ggplot(df.new[[2]], aes(x=v, y=Custo)) +
134   geom_line(aes(colour="Exact Cost")) +
135   geom_line(aes(x=v, y=Linf, colour="Lower Bound")) +
136   geom_line(aes(x=v, y=Lsup, colour="Upper Bound")) +
137   scale_colour_manual("", values=c("Exact Cost"="black", "Lower Bound"=
138     "red", "Upper Bound"="blue")) +
139   labs(x="n",
140         y="Cost",
141         title=expression(paste(lambda[1]==0.95, "and ", lambda[2]==0.92)))
142   ) +
143   theme(legend.background=element_rect(fill = alpha("white", 0)),
144         legend.key=element_rect(fill = alpha("white", .5))) +
145   theme(legend.position = c(0.81, 0.16),
146         legend.text = element_text(size = 6),
147         legend.background = element_rect(size=0.3),
148         plot.title = element_text(size=8, hjust=0.5),
149         axis.text = element_text(size = 7),
150         axis.title = element_text(size= 7))
151 library(gridExtra)
152 n <- length(graf)
153 nCol <- floor(sqrt(n))
154 do.call("grid.arrange", c(graf, ncol=nCol))
155 #install.packages("ggbpubr", dependencies=TRUE)

```

```

154 library(ggpubr)
155 gg<-ggarrange(p1, p2, p3, p4, ncol=2, nrow=2, common.legend = TRUE,
156   legend="bottom")
157 geom_point(shape=1,size=0.8,
158   aes(colour="Sample Cost",shape="Sample Cost",linetype="
159     Sample Cost"))+
160   stat_function(fun=function(x) C_Teo,
161   aes(colour="Expected Cost",shape="Expected Cost",linetype=
162     "Expected Cost"))+
163   scale_colour_manual('',values=c("Sample Cost"="black","Expected
164     Cost"="red"))+
165   scale_shape_manual('',values=c("Sample Cost"=1,"Expected Cost"=NA))
166   +
167   scale_linetype_manual('',values=c("Sample Cost"=0,"Expected Cost"
168     =1))+ 
169   labs( x="m ( n=10 )", y="Cost", title = "Convergence of Sample
170     Minimum Cost")+
171   theme(legend.position = c(0.81, 0.16),
172     legend.text = element_text(size = 5),
173     legend.title = element_blank(),
174     legend.background = element_rect(size=0.3),
175     plot.title = element_text(size=8,hjust=0.5),
176     axis.text = element_text(size = 7),
177     axis.title = element_text(size= 7))
178 #=====
179 #=====DISTRIBUICAO EMPIRICA DO CUSTO=====#
180 #=====#
181 ## R Base

```

```

175 n<-100:120 ; l1<-c(2,4,6,8) ; l2<-c(2,3,5,7)
176 set.seed(12345) ; par(mfrow=c(2,2))
177 for (i in 1:4) {
178   plot.ecdf(Custo_teorico(n,l1[i],l2[i]),main="Distribuicao Empirica
179     do Custo Esperado")
180   legend("topleft",legend=bquote(lambda[1]==.(l1[[i]]) ~ " , " ~ lambda
181     [2]==.(l2[[i]])))
182 }
183 Var_Custo.est<-function(n,m,l1,l2) { (n*(n+1)/(2*m))*(1/l1^2+1/l2^2)}
184 set.seed(12345)
185 par(mfrow=c(1,1))
186 l1<-0.55 ; l2<-0.95 ; m<-40:2000
187 Custo.est<-function(n,m,l1,l2) {
188   # l1: taxa do processo 1
189   # l2: taxa do processo 2
190   # n: quantidade de amostras de tempo; (n primeiras chegadas)
191   # m: tamanho de cada amostra do tempo X_i
192   Custo<-numeric(length(n))
193   for (j in 1:length(n)) {
194     mat.X<-matrix(0,nrow=n[j],ncol=m)
195     mat.Y<-matrix(0,nrow=n[j],ncol=m)
196     for (i in 1:n[j]) {
197       mat.X[i,]<-rgamma(m,i,l1) # m tempos do 1o processo
198       mat.Y[i,]<-rgamma(m,i,l2) # m tempos do 2o processo
199     }
200     Custo[j]<-sum(rowMeans(abs(mat.X-mat.Y)))
201   }
202   return(Custo)

```

```

201 }
202 #=====
203 #===== CONVERGENCIA DO CUSTO =====#
204 #=====
205 C_est<-sapply(m,Custo.est,n=10,11,12)
206 C_Teo<-Custo_teorico(10,11,12)
207 ### Grafico no R Base
208 x11()
209 plot(m,C_est,xlab="m (n=10)",ylab="Cost",cex.axis=0.6,cex.lab=.7,
210      mgp=c(1.2,0.5,0), cex=0.6, tck=0.02, )
211 legend("bottomright",inset=0.02,legend=c("Expected Cost", "Sample Cost
212      "),
213      col=c("red", "black"),lty=c(1,1),cex=0.4)
214 abline(h=C_Teo,col="red")
215 title(main="Convergence of Sample Minimum Cost",cex.main=0.62)
216 ### Grafico no ggplot2
217 library(ggplot2)
218 df2<-data.frame(m,C_est)
219 g2<-ggplot(data=df2, aes(x=m, y=C_est))+geom_point(shape=1,size=0.8,aes(colour="Sample Cost",shape="
220      "Sample Cost",linetype="Sample Cost"))+
221      stat_function(fun=function(x) C_Teo,aes(colour="
222      "Expected Cost",shape="Expected Cost",linetype="
223      "Expected Cost"))+
224      scale_colour_manual('' ,values=c("Sample Cost"="black"
225      ,"Expected Cost"="red"))+
226      scale_shape_manual('' ,values=c("Sample Cost"=1,"
227      "Expected Cost"=NA))+

```

```

223     scale_linetype_manual('', values=c("Sample Cost"=0,
224                               "Expected Cost"=1))+  

225     labs( x="m ( n=10 )", y="Cost", title = "Convergence  

226           of Sample Minimum Cost")+
227     theme(legend.position = c(0.81, 0.16),  

228           legend.text = element_text(size = 5),  

229           legend.title = element_blank(),  

230           legend.background = element_rect(size=0.3),  

231           plot.title = element_text(size=8,hjust=0.5),  

232           axis.text = element_text(size = 7),  

233           axis.title = element_text(size= 7))  

234 #=====  

235 #=====CUSTO ESPERADO x CUSTO AMOSTRAL=====#
236 #=====  

237 l1<-0.95 ; l2<-0.90  

238 n<-100:130  

239 CUSTO<-sapply(n,Custo.teorico,l1=l1,l2=l2)  

240 set.seed(12345)  

241 CUSTO.est<-sapply(n,Custo.est,m=100,l1=l1,l2=l2)  

242 plot(n,CUSTO.est,type="l",ylab="Custo",xlab="n (m=100)")  

243 lines(n,CUSTO,col="red")  

244 title(main="Custo Esperado X Custo Amostral")  

245 legend("topleft", expression(lambda[1]~"= 0.95, " ~lambda[2]~" = 0.90"  

246 ))  

247 legend("bottomright",inset=0.02,legend=c("Custo Esperado", "Custo  

248 Amostral"),  

249 col=c("red","black"),lty=c(1,1),cex=0.8)  

250 x11(width=3.8,height=2.9)

```

```

247 plot(n,CUSTO.est,pch=1,ylab="Cost",xlab="n (m=100)",
248     main = "Expected Cost X Sample Cost",
249     cex.lab= 0.7,
250     cex.axis=0.5,
251     cex.main=0.7,
252     mgp=c(1.2,0.5,0), cex=0.6,
253 )
254 lines(n,CUSTO, col="red")
255 df1<-data.frame(n,CUSTO,CUSTO.est)
256 dev.off()
257 g1<-ggplot(data=df1, aes(x=n, y= CUSTO.est))+
258   geom_point(shape=1,size=1,aes(colour="Sample Cost",shape="Sample
259   Cost",linetype="Sample Cost"))+
260   geom_line(aes(x=n, y= CUSTO, shape="Expected Cost", colour="
261   Expected Cost",linetype="Expected Cost"))+
262   scale_colour_manual('',values=c("Sample Cost"= "black", "Expected
263   Cost"="red"))+
264   scale_shape_manual('',values=c("Sample Cost"=1, "Expected Cost"=
NA)
265   )+
266   scale_linetype_manual('',values=c("Sample Cost"=0, "Expected Cost"
267   =1))+

268 labs( x="n ( m=100 )", y="Cost", title = "Expected Cost X Sample
269   Cost")+
270 theme(legend.position = c(0.81, 0.16),
271       legend.text = element_text(size = 5),
272       legend.title = element_blank(),
273       legend.background = element_rect(size=0.3),
274       plot.title = element_text(size=8,hjust=0.5),

```

```

269     axis.text = element_text(size = 7),
270     axis.title = element_text(size= 7))
271 setwd("C:/Users/adolfoamds/Documents")
272 path<-getwd()
273 ggsave(filename="convergen.pdf", plot=g1, device="pdf",
274         path=path, height=3.0, width=3.2, units="in", dpi=500)
275 #=====
276 #===== GRAFICO AJUSTE DA NORMAL =====#
277 #=====
278 Q_Pivo<-function(n,m,l1,l2){
279   res<-(Custo.est(n,m,l1,l2) - Custo_teorico(n,l1,l2))/sqrt(Var_Custo
280   .est(n,m,l1,l2))
281   return(res)
282 }
283 Qtd_Pivotal<-sapply(100:1000,Q_Pivo,m=100,l1=0.95,l2=0.90)
284 #install.packages("fitdistrplus")
285 library(fitdistrplus)
286 ajuste_normal<-fitdist(Qtd_Pivotal,"norm")
287 x11(width = 3.8, height=5)
288 plot(ajuste_normal,cex.main=0.75,cex=0.4,cex.lab=.7,cex.axis=0.7)
289 #install.packages("ggplot2") ; install.packages("gridExtra")
290 library(ggplot2)
291 ## Intervalo de Confianca ao nivel de 95%
292 Intervalo<-function(n,m,l1,l2){
293   int<-Custo.est(n,m,l1,l2)+c(-1,1)*qnorm(0.975)*sqrt(Var_Custo.est(n,
294   m,l1,l2))
295   return( int )
296 }
```

```

295 set.seed(12345) ; n<-1200:1250
296 Int<-sapply(n, Intervalo, m=100, l1=0.95, l2=0.9)
297 LI<-Int[1,]
298 LS<-Int[2,]
299 CUSTO<-sapply(n, Custo_teorico, l1=0.95, l2=0.90)
300 df0 <- data.frame( n = n,
301                      custo = CUSTO,
302                      li = LI,
303                      ls = LS
304 )
305 grafico0<-ggplot(df0, aes(n, custo)) +
306   geom_point() +
307   geom_line() +
308   geom_errorbar(aes(ymin = li, ymax = ls)) +
309   labs(x = "n ( m=100 )",
310        y = "Cost",
311        title = "Expected Minimum Cost and 95% CI") +
312   theme( plot.title = element_text(size=11) )
313 path<-getwd()
314 ggsave(filename="gg-formatted.png", plot=grafico0, device="png",
315         path=path, height=3.5, width=4, units="in", dpi=500)
316 N<-rep(n, 3)
317 Custo<-c(LS, CUSTO, LI)
318 Legenda<-rep( c("Upper Bound", "Expected Cost", "Lower Bound"), each=
319   length(n))
320 df<-data.frame(n=N, Legenda, Custo)
321 grafic01<-ggplot(df, aes(x = n, y = Custo)) +
322   geom_line(aes(color = Legenda, linetype = Legenda)) +

```

```

322 scale_color_manual(values = c("red", "black", "blue")) +
323   labs( x="n ( m=100 )", y="Cost",
324         title = "Expected Minimum Cost and 95% CI") +
325   theme(legend.position = c(0.80, 0.22),
326         legend.text = element_text(size = 6),
327         legend.title = element_blank(),
328         legend.background = element_rect(size=0.3),
329         plot.title = element_text(size=8,hjust=0.5),
330         axis.text = element_text(size = 7),
331         axis.title = element_text(size= 7))
332 path<-getwd()
333 ggsave(filename="Afvbogg.pdf", plot=graficol, device="pdf",
334         path=path, height=3, width=3.5, units="in",dpi=500)
335 gridExtra::grid.arrange(grafico0, graficol, ncol=2)
336 INT <- function(n,m,l1,l2,cl) {
337   # cl: nivel de confianca
338   alpha <- 1-cl/100
339   # CI para Custo Teorico (Esperado)
340   dp_am <-sqrt(Var_Custo.est(n,m,l1,l2))      # desvio padrao amostral
341   z_s <- qnorm(1 - alpha/2)                      # quantil da normal
342   li <- Custo.est(n,m,l1,l2) - z_s*dp_am       # limite inferior
343   ls <- Custo.est(n,m,l1,l2) + z_s*dp_am       # limite superior
344   c(limite_Inferior=li, limite_superior=ls)
345 }
346 # Gerar N vezes os Intervalos para Custo Teorico
347 simulacao <- function(N,n,m,l1,l2,cl) {
348   set.seed(123)
349   sim<-t(replicate(N, INT(n,m,l1,l2,cl)))

```

```

350 return(list("Qtd de Intervalos que Contem o Custo"=
351             N*mean(sim[,1] <= Custo_teorico(n,11,12) &
352                     sim[,2]>= Custo_teorico(n,11,12)), "Total de
353                     Intervalos"=N))
354 }
354 #===== CHAPTER 3 =====#
355 #===== a-th moment by Kapelko (2017) =====#
356 #=====
357 E<-function(a,k,l) {
358   nnn(gamma(a+1)/l^a)*( gamma(a/2+k) / (gamma(k)*gamma(a/2+1)) ) }
359 #=====
360 #=====Gauss hypergeometric function=====
361 #=====
362 ## used packages: "gsl"
363 #install.packages("gsl")
364 library(gsl)
365 Gauss2F1 <- function(a,b,c,z) {
366   if(z>=0 & z<1) {
367     hyperg_2F1(a,b,c,z)
368   }else{
369     hyperg_2F1(a,c-b,c,1-1/(1-z))/(1-z)^a
370   }
371 }
372 #=====
373 #===== Pochhammer polynomial =====#
374 #=====
375 p.c <- function( x, q ){
376   if ( q < 0 )

```

```

377     stop( "q e negativo" )
378
379 else if ( q == 0 )
380
381     return ( 1 )
382
383 else {
384
385     res <- 1
386
387     for ( i in 1:q ) {
388
389         res <- res * ( x + i - 1 )
390
391     }
392
393     return ( res )
394
395 }
396
397 return ( NULL )
398
399 }
400
401 #### generalized moment function #####
402 #### Parameters:
403 # a := order of the moment
404 # k := arrival time order
405 # r := lag between times
406 # l1 := first process arrival rate
407 # l2 := second process arrival rate
408 Mg<-function(a,k,r,l1,l2){
409
410 I_1<-NULL ; I_2<-NULL
411
412 for (i in 1:length(l1)) {
413
414 f<-function(j){(factorial(a)*(-1)^a/l2[i]^a)*(p.c(k+r,j)*p.c(k,a-j)
415
416 /(factorial(j)*factorial(a-j)))*(-l2[i]/l1[i])^j}
417
418 j<-0:a
419
420 I_1[i]<-sum(sapply(j,f))

```

```

404 I_2[i] <- ((l1[i]/l2[i])^(k+r)*l2[i]^(-a)*gamma(a+1)*(-1)^a*gamma(a
405   +2*k+r)/(gamma(k)*gamma(1+k+r+a)))*Gauss2F1(a+2*k+r,k+r,1+k+r+a
406   ,-l1[i]/l2[i])
407 }
408
409 return(I_1-2*I_2*ifelse(a%%2==1,1,0))
410 }
411 #=====
412 #=====programming code for corollaries 1 and 2 (Kapelko (2017))=====
413 #=====
414 ## Parameters:
415 # a := order of the moment
416 # k := arrival time order
417 # l := rate of arrival
418 E1<-function(a,k,l){
419   res<-NULL
420   for (i in 1:length(l)){
421     res[i]<-(gamma(a+1)/l[i]^a)*(gamma(a/2+k)/(gamma(k)*gamma(a/2+1)))
422   }
423   return(res)
424 }
425 #=====
426 #=====programming code for graphics=====
427 #=====plot function for graphic 1=====
428 ## used packages: "gridExtra" ; "ggplot2" ; "Plot3D"
429 #install.packages("gridExtra") ; install.packages("ggplot2")
430 library(ggplot2) ; require(gridExtra)
431 ## Parameters:
432 # n:= n first moments

```

```

430 # k:= arrival time order
431 # l_in := start rate
432 # l_fin := end rate
433 # comp := number of rates between l_in and l_fim
434 # curve := 0 (detach); 1 (joins)
435 g2<-function(n, k, l_in, l_fim, comp, curve) {
436   v<-seq(l_in,l_fim,length.out=comp)
437   a<-(1:n)
438   arg3<-rep(v,length(a))
439   arg1<-rep(a,each=length(v))
440   arg2<-rep(k,length(a)*length(v))
441   y<-mapply(E2,arg1,arg2,0,arg3,arg3) ; arg1<-as.factor(arg1)
442   dd<-data.frame(x=arg3,y=y,a=arg1)
443   if( curva==0) {
444     ggplot(data=dd,aes( x=x, y=y, color=a)) +
445       geom_line() + facet_wrap(~ a)+ylim(0,50) +
446       labs(x=expression(lambda),y=expression(M[pop]^a)) +
447       theme(plot.title=element_text(size=7, face="bold",
448                                     color="black",hjust=0.5),
449             axis.text=element_text(size=7))
450   } else {
451     ggplot(data=dd,aes( x=x, y=y, color=a)) +
452       geom_line() +ylim(0,50) +
453       labs(x=expression(lambda),y=expression(M[pop]^a)) +
454       theme(plot.title=element_text(size=9,face="bold",
455                                     color="black",hjust=0.5)) }
456   }
457 x11()

```

```

458 grid.arrange(g2(9,2,0.1,5,1000,0) , g2(9,2,0.1,5,1000,1),nrow=2)
459 #===== plot function for graphic 2 =====#
460 ### used packages: "plot3D"
461 install.packages("plot3D") ; library(plot3D)
462 l1<-sort(runif(100,2,5)) ; l2<-l1
463 dd<-data.frame(x=l1,y=l2,e1=E2(1,4,0,11,12),e2=E2(2,4,0,11,12),
464 e3=E2(3,4,0,11,12),e4=E2(4,4,0,11,12) )
465 par(mfrow=c(2,2))
466 for (i in 3:6){
467   x11()
468   scatter3D(l1,l2,dd[,i],phi=0,type="h",bty="g",ticktype="detailed",
469   ,pch=19,cex=0.5,main="",xlab="",ylab="",zlab= "", colkey =
470   list(length = 0.5, width = 0.5, cex.lab = 0.5, side=1))
471   text3D(-14,7,0.7, labels = expression(M[pop]^a), add = TRUE)
472   text3D(3.5,1.2,0.4, labels = expression(lambda[1]), add = TRUE)
473   text3D(5.7,3.0,0.4, labels = expression(lambda[2]), add = TRUE)
474 }
475 #=====plot function for graphic 3=====#
476 ### used packages: "Plot3D"
477 library(plot3D)
478 l1<-runif(500,2,6) ; l2<-runif(500,2,6)
479 dd<-data.frame(x=l1,y=l2,e1=E2(1,4,0,11,12),e2=E2(2,4,0,11,12),
480 e3=E2(3,4,0,11,12),e4=E2(4,4,0,11,12) ) ; par(mfrow=c
481 (2,2))
482 for (i in 3:6){
483   x11()
484   scatter3D(l1,l2,dd[,i],phi=0, type="p",bty="g",ticktype="detailed",
485   pch=19,cex=0.7,main="",xlab="",ylab="",zlab= "",
```

```

483         colkey = list(length = 0.5, width = 0.5, cex.lab =0.5,
484                         side=1))

485     text3D(-14,7,0.7, labels = expression(M[pop]^a), add = TRUE)
486     text3D(5.0,0.8,0.4, labels = expression(lambda[1]), add = TRUE)
487     text3D(6.5,2.0,0.4, labels = expression(lambda[2]), add = TRUE)
488 }
489 #===== programming code for simulation =====#
490 ## Parameters:
491 # n := sample size
492 # a := order of the moment
493 # k := arrival time order
494 # r := lag between times
495 # l1 := first process arrival rate
496 # l2 := second process arrival rate
497 simula <- function(n,a,k,r,l1,l2){

498     Dif<-matrix(0,nrow=length(k),ncol=length(a))
499     Mom<-matrix(0,nrow=length(k),ncol=2*length(a))
500     colnames(Dif)<-rep("",length(a)) ; colnames(Mom)<-rep("",

501                                         ,2*length(a))

502     for (i in 1:length(k)){
503         X<-rgamma(n,k[i]+r[i],l1) ; Y<-rgamma(n,k[i],l2)

504         for (j in 1:length(a)){
505             Mom[i,2*j-1]<-E2(a[j],k[i]+r[i],0,l1,l2)

506             Mom[i,2*j]<-mean((abs(X-Y))^a[j])

507             Dif[i,j]<- Mom[i,2*j-1] - Mom[i,2*j]

508             colnames(Dif)[j]<-paste("D",j)

509             colnames(Mom)[2*j-1]<-paste("Mp",j)

510             colnames(Mom)[2*j]<-paste("Ma",j)

```

```
509         }
510     }
511     return(list(Moments=cbind(k,r,trunc(Mom,prec=4)),
512                  Moments_Difference=cbind(k,r,trunc(Dif,prec=4)) )))
513 }
514 ## Simulation 1
515 simula(1000000,1:4,1:12,rep(0,12),2,2)
516 ## Simulation 2
517 simula(10000000,1:4,1:12,rep(0,12),10,20)
```


Bibliography

- Ajtai, M., J. Komlós, and G. Tusnády (1984). “On optimal matchings”. *Combinatorica* 4.4, pp. 259–264.
- Augie, B. (2017). *gridExtra: Miscellaneous Functions for "Grid" Graphics*. R package version 2.3. URL: <https://CRAN.R-project.org/package=gridExtra>.
- Billingsley, P. (1995). *Probability and Measure*. John Wiley & Sons,
- DiDonato, A. and M. Jarnagin (1966). *A Method for computing the incomplete beta function ratio. Revised*. Tech. rep. Naval Weapons Lab Dahlgren VA.
- Feller, W. (1968). *An Introduction to Probability Theory and Its Applications. Vol. 1*. John Wiley & Sons,
- Fox, C. (1961). “The G and H functions as symmetrical Fourier kernels”. *Transactions of the American Mathematical Society* 98.3, pp. 395–429.
- Gould, H. W. (1972). *Combinatorial Identities: A standardized set of tables listing 500 binomial coefficient summations*. Gould.
- Gradshteyn, I. S. and I. M. Ryzhik (2014). *Table of integrals, series, and products*. Academic press.
- Kapelko, R. (2017). “On the expected moments between two identical random processes with application to sensor network”. *arXiv preprint arXiv:1705.08855*.
- Kapelko, R. (2018). “On the moment distance of Poisson processes”. *Communications in Statistics- Theory and Methods* 47.24, pp. 6052–6063.

- Kapelko, R. (2020). “On the Energy in Displacement of Random Sensors for Connectivity and Interference”. *Proceedings of the 21st International Conference on Distributed Computing and Networking*, pp. 1–10.
- Kapelko, R. (2015). “The weighted event distance of Poisson processes”. *arXiv preprint: 1507.01048*.
- Kranakis, E. (2014). “On the event distance of Poisson processes with applications to sensors”. *Discrete Applied Mathematics* 179, pp. 152–162.
- Kranakis, E. et al. (2013). “Expected Sum and Maximum of Displacement of Random Sensors for Coverage of a Domain: Extended Abstract”. *Proceedings of the Twenty-Fifth Annual ACM Symposium on Parallelism in Algorithms and Architectures*. SPAA ’13. Montréal, Québec, Canada: Association for Computing Machinery, 73–82.
- Ma, Z. et al. (2020). “Energy-efficient non-linear k-barrier coverage in mobile sensor network”. *Computer Science and Information Systems*, pp. 18–18.
- Mathai, A. M., R. K. Saxena, and H. J. Haubold (2010). *The H-function: theory and applications*. Springer Science & Business Media.
- Moltchanov, D. (2012). “Distance distributions in random networks”. *Ad Hoc Networks* 10.6, pp. 1146 –1166.
- Mondal, N. and P. P. Ghosh (2013). “Another Asymptotic Notation:” Almost””. *arXiv preprint arXiv:1304.5617*.
- Oliveira, E Capelas de (2012). *Funções Especiais com Aplicações*. Editora Livraria da Física - São Paulo.
- Pearson, K. (1948). *Tables of the Incomplete Beta-function*. Biometrika.
- Pérez, C. A. et al. (2011). “A system for monitoring marine environments based on Wireless Sensor Networks”. *OCEANS 2011 IEEE - Spain*, pp. 1–6. DOI: 10 . 1109 / Oceans - Spain.2011.6003584.
- R Core Team (2020). *R: A Language and Environment for Statistical Computing*. R Foundation for Statistical Computing. Vienna, Austria. URL: <https://www.R-project.org/>.

- RStudio Team (2020). *RStudio: Integrated Development Environment for R*. RStudio, PBC. Boston, MA. URL: <http://www.rstudio.com/>.
- Soetaert, K. (2019). *plot3D: Plotting Multi-Dimensional Data*. R package version 1.3. URL: <https://CRAN.R-project.org/package=plot3D>.
- Srivastava, H. E. (2019). *Mathematical Analysis and Applications*. Printed Edition of the Special Issue, Published in Axioms; MDPI Publishers; Basel, Switzerland.
- Teng, J. et al. (2007). “Sensor Relocation with Mobile Sensors: Design, Implementation, and Evaluation”. *2007 IEEE International Conference on Mobile Adhoc and Sensor Systems*, pp. 1–9. DOI: [10.1109/MOBHOC.2007.4428666](https://doi.org/10.1109/MOBHOC.2007.4428666).
- Titchmarsh, E. (1986). *Introduction to the Theory of Fourier Transforms*. Oxford University Press. Oxford.
- Tudose, D. et al. (2011). “Mobile sensors in air pollution measurement”. *2011 8th Workshop on Positioning, Navigation and Communication*, pp. 166–170. DOI: [10.1109/WPNC.2011.5961035](https://doi.org/10.1109/WPNC.2011.5961035).
- Wickham, H. (2016). *ggplot2: Elegant Graphics for Data Analysis*. Springer-Verlag New York. ISBN: 978-3-319-24277-4. URL: <https://ggplot2.tidyverse.org>.